UNIVERSIDADE
BEIRA INTERIOR

Development of cationic polymeric nanoparticles for plasmid DNA vaccine delivery

Renato Pereira Nunes

Dissertação para obtenção do Grau de Mestre em
Bioengenharia
2º ciclo de estudos

Orientador: Prof. Doutor Ângela Maria Almeida de Sousa
Co-orientador: Prof. Doutor Aiva Simaite

Junho de 2021

Acknowledgments

First of all, thank my family for the support during these years I lived abroad far away from them, for always believe and never give up on me. To my parents, Fernando Nunes and Gildete Nunes, my brother Fernando Filho. No words I write here will be enough to thank them. They know how gratified I am for all the efforts, education, loyalty, affection, and love, thank you!

I thank the University of Beira Interior, especially the Health Science Research Centre, and the bio/nano technology company InoCure, based in Prague, Czech Republic, where I spent one year learning all the skills needed for the development of this thesis. For both institutions, I would like to thank the laboratory equipment and materials available. Thanks to all researchers of both organizations center, particularly to my supervisor and co-supervisor Ângela Sousa and Aiva Simaite, respectively. They contributed to a better work environment and gave me all the support needed, without the vast knowledge of both this work could not be done.

Resumo

O cancro é a segunda causa de morte mais prevalente no mundo e ainda não tem cura universal. O papilomavírus humano (HPV) está entre os principais patógenos carcinogénicos e a sua infecção está relacionada com diversos tipos de cancro, como cancro do colo do útero e orofaríngeo. O cancro do colo do útero é a quarta maior causa de cancro em mulheres em todo o mundo. Atualmente é considerado um dos problemas mais comuns de saúde pública, principalmente no grupo de mulheres de meia-idade, principalmente nos países menos desenvolvidos. Os dois principais genótipos infecciosos do papilomavirus são HPV16 e HPV18, e são considerados os mais oncogénicos e responsáveis por mais de 70% dos cancros de colo do útero.

Entre as oncoproteínas do vírus HPV a oncoproteína E7 inibe a atividade da proteína retinoblastoma (pRb), levando à desregulação do ciclo celular e consequente crescimento descontrolado de células. A vacinação é considerada a maior contribuição para as intervenções de saúde pública global dos últimos séculos. A evolução e consequente contribuição das vacinas são responsáveis por um aumento assentuado da expectativa geral de vida. No entanto, as vacinas atuais contra o vírus do HPV não têm efeito terapêutico quando o paciente já está infectado. Isso significa que a vacina só pode prevenir a infecção pelo HPV, mas não pode tratar ou reverter os cancros induzidos por infecções por HPV pré-existentes e persistentes. Dessa forma, as vacinas de DNA podem ser uma solução promissora para o tratamento eficaz de indivíduos infectados pelo HPV, uma vez que podem induzir respostas imunes preventivas e terapêuticas. Para ser eficaz, o DNA precisa ser internalizado no núcleo da célula eucariótica sem degradação e a expressão do gene alvo também depende da não degradação da molécula de DNA. Porém, a eficiência de internalização é baixa, devido à repulsão do DNA pela membrana. A administração intramuscular é uma das principais vias de administração da vacina de DNA. No entanto, requer grandes quantidades de DNA a ser administrado e estimulação externa para aumentar a internalização do DNA nas células eucarióticas.

Neste trabalho, consideramos sistemas de entrega de fármacos biocompatíveis que irão proteger, transportar e auxiliar a internalização celular das vacinas de DNA. Isto pode oferecer uma via de administração alternativa e menos invasiva, como a administração intranasal. Neste contexto, poliplexos de quitosano usando tripolifosfato de sódio (TPP) como um agente reticulante foram desenvolvidos e aperfeiçoados usando o método de gelificação ionotrópica. Vários parâmetros que podem afetar a formulação do sistema

foram investigados, incluindo diferentes volumes e concentrações de TPP e quitosano, concentrações de DNA, taxa de fluxo de adição de solução de TPP/DNA/pDNA. Esses nano-transportadores foram caracterizados em termos de tamanho, carga de superfície, eficiência de encapsulação, morfologia, estabilidade, viabilidade celular explorando duas linhagens celulares diferentes. Por fim, a verificação da internalização celular e consequente expressão do gene alvo codificado na vacina de DNA também foi verificada pelas técnicas de *reverse transcription polymerase chain reaction* (RT-PCR) e *reverse transcription-quantitative real-time* (RT-qPCR).

Os resultados mostraram que a variação dos parâmetros permitiu superar um desafio comum em relação aos sistemas de quitosano, obtendo nanopartículas monodispersas com tamanhos reduzidos, abaixo de 200nm, e eficiência de encapsulação superior a 60%. As nanopartículas analisadas por microscopia eletrónica de varrimento apresentam formas esféricas ou ovais em nano tamanhos. Estudos de estabilidade demonstraram que os poliplexos são capazes de proteger o DNA encapsulado de proteases, tripsina, meio DMEM-F12 suplementado com 10% de soro fetal bovino e meio de Eagle modificado por Dulbecco com alta glicose (DMEM-HG) suplementado com 10% de soro fetal bovino não inativado. O ensaio de resazurina mostrou que os sistemas são biocompatíveis, garantindo que nenhuma citotoxicidade será induzida. Além disso, os resultados de PCR e RT-qPCR mostraram que as nanopartículas produzidas têm o efeito desejado e pretendido, mostrando que são adequadas para captação celular, internalização e expressão génica.

Em conclusão, os resultados apresentados revelaram que os poliplexos quitosano-TPP-pDNA são adequados como um bom nano-transportador para a entrega de vacina de DNA plasmídico.

Palavras-chave

Gelificação ionotrópica; infecção do HPV; nanopartículas; quitosano; vacinas de DNA plasmídico.

Abstract

Cancer is the second most prevalent cause of death in the world and does not yet have a universal cure. Human papillomavirus (HPV) is among the main carcinogenic pathogens and its infection is related to several cancers, such as cervical and oropharyngeal cancers. Cervical cancer is the 4th largest cause of cancer in women worldwide. Nowadays it is considered one of the most common public health issue, principally in middle-aged women group, especially in less developed countries. The two major infectious papillomavirus genotypes are HPV16 and HPV18, and they are considered to be the most oncogenic and responsible for more than 70% of cervical cancers.

Among the HPV virus oncoproteins the E7 oncoprotein inhibits the activity of the retinoblastoma protein (pRb), leading to a deregulation of the cell cycle and consequent uncontrolled growth of cells. Vaccination is considered to be the greatest contribution to global public health interventions of the latest centuries. The evolution and consequent contribution of vaccines are responsible for an impressive increase in general life expectancy. However, the current vaccines against the HPV do not have a therapeutic effect when the patient is already infected. This means that the vaccine can only prevent the infection by the HPV, but cannot treat or revert cancers induced by pre-existing and persistent HPV infections. In this way, DNA vaccines can be a promising solution for the effective treatment of HPV-infected individuals, since they can induce preventive and therapeutic immune responses. In order to be effective, the naked DNA needs to be internalized into the eukaryotic cell nucleus without degradation and the target gene expression is also dependent on the non-degradation of the DNA molecule. However, the internalization efficiency is low, due to the repulsion of the DNA by the membrane. Intramuscular delivery is one of the main routes for DNA vaccine administration. Nevertheless, it requires large amounts of the DNA administered and external stimulation to encourage the internalization of the DNA into the eukaryotic cells. In this work, we consider biocompatible drug delivery systems that can protect, carry and help the cellular internalization of DNA vaccines. This can lead to alternative and less invasive administration routes, such as intranasal administration.

In this context, Chitosan (CS) polyplexes using sodium tripolyphosphate (TPP) as a crosslinker were designed and prepared using the ionotropic gelation method. Several parameters that may affect the systems formulation were investigated, including different TPP and CS volumes and concentrations, DNA concentrations, flow rate speed

addition of TPP/DNA/pDNA solution. These nanocarriers were characterized in terms of size, surface charge, encapsulation efficiency, morphology, stability and cellular viability exploring two different cell lines. Ultimately, the verification of cell internalization and consequent target gene expression encoded in the DNA vaccine was also verified by *reverse transcription polymerase chain reaction* (RT-PCR) and *reverse transcription-quantitative real-time*.

The results showed that the variation of parameters allowed to overcome an ordinary challenge regarding the CS systems achieving monodisperse nanoparticles (NPs) with good size, bellow 200 nm and encapsulation efficiency higher than 60%. The nanoparticles analyzed by scanning electron microscopy (SEM) present spherical or oval shapes in nano sizes. Stability studies demonstrated that the polyplexes are able to protect encapsulated DNA from serine proteases, trypsin, DMEM-F12 medium supplemented with 10% of fetal bovine serum, and Dulbecco´s Modified Eagle´s Medium with High Glucose (DMEM-HG) supplemented with 10% not inactivated fetal bovine serum. Resazurin assay showed that the systems are biocompatible supporting that no cytotoxicity is induced. In addition, the PCR and RT-qPCR results showed that produced nanoparticles have the desired and intended effect, showing that they are suitable for cell uptake, internalization, and gene expression.

In conclusion, the presented results revealed that the CS-TPP-pDNA polyplexes are suitable as a good nanocarrier for plasmid DNA vaccine delivery.

Keywords

Ionotropic gelation; Chitosan; HPV infection; nanoparticles; pDNA vaccines.

Index

List of Figures

List of Tables

List of Abbreviations

APCs: Antigen-presenting cells
CICS: Health Sciences Research Centre
CR: Conserved regions
CS: Chitosan
CTLs: Cytotoxic T Lymphocyte
DDA: Deacetylation degree
dEE: Direct encapsulation efficiency
DEPC: Diethylpyrocarbonate
DLS: Dynamic Light Scattering
DMEM: Dulbecco´s Modified Eagle´s Medium
DMEM-HG: Dulbecco´s Modified Eagle Medium - High glucose
DNA: Deoxyribonucleic acid
dsDNA: Double-stranded DNA
E. coli: Escherichia coli
E6AP: E6 Associated protein
EDTA: Ethylenediamine tetraacetic acid
EE: Encapsulation Efficiency
EMA: European Medicines Agency
FBS: Fetal bovine serum
FDA: Food and Drug Administration
FW: Forward
gDNA: Genomic DNA
GHRH: Growth hormone-releasing hormone
GIT: Gastrointestinal tract
HMW: High molecular weight
HPV: Human papillomavirus
HR-HPV: High-risk HPV
IECP: International Electronic Conference on Pharmaceutics
iEE: Indirect encapsulation efficiency
kb: Kilobase
kbp: Kilobase pair
LB: Luria-Bertani
LCR: Long Control Region
MAPs: Mucoadhesive particles

MDPI: Multidisciplinary Digital Publishing Institute

MHC: Major histocompatibility complex

MM: Molar Mass

MMW: Medium molecular weight

mRNA: Messenger RNA

MRT: Mean residence time

Mw: Molecular weight

N: Amine groups

NPs: Nanoparticles

o/w: Oil / water

ºC: Degree Celsius

OD: Optic density

ODd: Desired optic density

ODp.i.: Pre-inoculum optic density

PDI: Polydispersive index

P: Phosphate groups

PBS: Phosphate buffer solution

pDNA: Plasmid DNA

PEI: Polyethyleneimine

pRb: Retinoblastoma protein

RCF: Relative centrifugal force

RNA: Ribonucleic acid

rpm: Revolutions per minute

RT-PCR: Reverse transcription polymerase chain reaction

RT-qPCR: Reverse transcription-quantitative real-time PCR

RV: reverse

SD: Standard deviation

SEM: Scanning electron microscopy

SLNs: Solid lipid nanoparticles

TAE: Tris-acetate-EDTA

TB: Terrific Broth

TEM: Transmission electron microscopy

TPP: Sodium tripolyphosphate

UBI: University of Beira Interior

UV: Ultraviolet

v/v %: Volume per volume percentage

Vf: Volume Fermentation

VLPs: Virus-like particles

w/v %: Weight per volume percentage

WHO: World Health Organization

List of Scientific Communications

Oral presentation

The 1st International Electronic Conference on Pharmaceutics (IECP 2020).

Presentation and video presentation are available for download at <https://sciforum.net/event/IECP2020/submissions/view>. (Consult annex 1)

List of Scientific Publications

Nunes, R.; Sousa, Â.; Simaite, A.; Aido, A.; Buzgo, M. Sub-100 nm Chitosan-Triphosphate-DNA Nanoparticles for Delivery of DNA Vaccines. *Proceedings* **2021**, *78*, 12. https://doi.org/10.3390/IECP2020-08653. (Consult annex 2)

Nunes, R.; Serra, A.; Simaite, A.; Sousa, Â; Design, formulation and characterization of chitosan polyplexes for plasmid DNA vaccine delivery. *Polymers* **2021**. (Manuscript in preparation).

1 Introduction

1.1 Cancer and Human Papillomavirus

Cancer is the second most prevalent cause of death in the world and does not yet have a universal cure. Human papillomavirus (HPV) is among the main carcinogenic pathogens and its infection is related to several cancers, such as cervical and oropharyngeal cancers (Nagai and Kim 2017; Doorbar et al. 2015). Cervical cancer is the 4th largest cause of cancer in women worldwide. Nowadays is considered one of the most common public health issue, principally in middle-aged women group, especially in less developed countries. Some specific actions have been made to reduce cervical cancer rates, such as sexual education campaigns by the government, improvement of HPV vaccination, easier access to cancer screening tests, and immunotherapy treatment (Arbyn et al. 2020). According to World Health Organization (WHO), HPV is also related to other less aggressive cancers of head, neck, anus, vulva, vagina, or penis. The transmission of the HPV virus is most related with sexual relationship. However, it is known that the simple contact between the genital organs is enough for the virus transmission (Doorbar et al. 2015).

1.1.2 HPV classification

There are more than 200 HPV genotypes identified. They are classified according to their oncogenic potential in low or high risk genotypes, as well as in genotypes of possible/probable high risk or indeterminate risk. High-risk HPV (HR-HPV) genotypes are the main ones responsible for cervical cancer cases, the most common are 16/18/31/33/35/39/45/51/52/56/58/59/66, and 68. The type 16 and 18 considered the most oncogenic among them. They can also be grouped into different genera (Alpha-, Nu-/Mu-, Beta- and Gamma-papillomavirus). The three main groups are gamma, alpha, and beta, respectively and together they are responsible for approximately 218 types of HPV, meanwhile, the other two groups for four types. The genera beta, gamma, mu, and nu contain HPV types that cause cutaneous infection, while the alpha is frequently related to benign genital warts and causes cutaneous, and mucosal infections (Sousa et al. 2019; Gheit 2019).

1.1.3 HPV genome organization

HPVs belong to the *papillomaviridae* family. These small and non-enveloped viruses have double-stranded circular DNA with a length that can range from 5 to 8 kbp. The

HPV genome is formed by three main regions according to their functional properties and location (Figure 1). The "Early" genes region (encoding E1, E2, E4, E5, E6, and E7 proteins) is responsible for regulatory functions associated with viral gene expression, replication, and survival. The "Late" genes region (encoding L1 and L2 proteins) is responsible for the virion assembly. The third region, named as Long Control Region (LCR), situated between L1 and E6 genes, contains the early promoter and is known as the region responsible for replication and transcription of viral DNA (Sousa et al. 2019; Gheit 2019; Viarisio, Gissmann, and Tommasino 2017; Payne 2017).

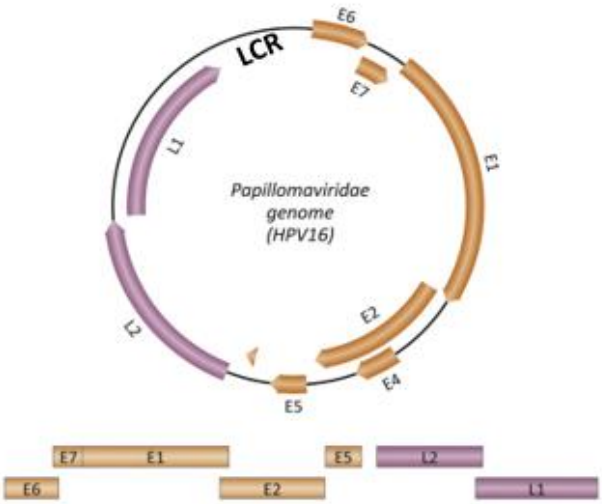

Figure 1. Genome organization of human papillomavirus 16 with the positions of "early" genes, "late" genes, and LCR (adapted from (Payne 2017)).

Figure 1 represents the eight major proteins and their location in the HPV genome. The six "early" genes are expressed in the beginning and, are responsible for genome maintenance and cellular proliferation, while the two "late" genes are expressed in the final stages of differentiation and consist of the virus capsid, which are important for the transmission, spread, and survival (Payne 2017; Graham 2010). The role and function of these proteins are depicted in table 1.

Table 1. Major role and function of the viral proteins in the HPV life cycle (adapted from (Viarisio, Gissmann, and Tommasino 2017; Graham 2010)).

Protein	Role and function in virus life cycle
E1	Viral replication: ATP-dependent DNA helicase. Forms a heterodimer complex with E2.
E2	Viral DNA replication, together with E1. Transcription, segregation, and encapsidation. Regulates early gene promoter/expression, cell cycle, and apoptosis.

E4	Responsible for the release of viral particles by destabilizing/remodeling the cytokeratin network. Cell cycle stopping point. Virion assembly.
E5	Control of cell growth and differentiation by stimulating mitogenic signals. Immune modulation.
E6	Oncoprotein. Inhibits apoptosis, differentiation, and inactivates many cellular proteins. Regulates cell shape, polarity, mobility, and signaling.
E7	Oncoprotein. Cell cycle control. Control centrosome duplication. Interacts with and inactivates many cellular proteins.
L1	The component of the HPV prophylactic vaccine. Major capsid protein.
L2	The minor capsid protein Recruits L1. Virus assembly.

1.1.4 HPV replication cycle

The replication cycle of HPV is connected to the differentiation of the epithelium, which does not suffer cell death after the infection. HPV infection generally happens at a site of epithelial abrasion (Roden and Stern 2018). A schematic design of HPV life cycle is shown in Figure 2.

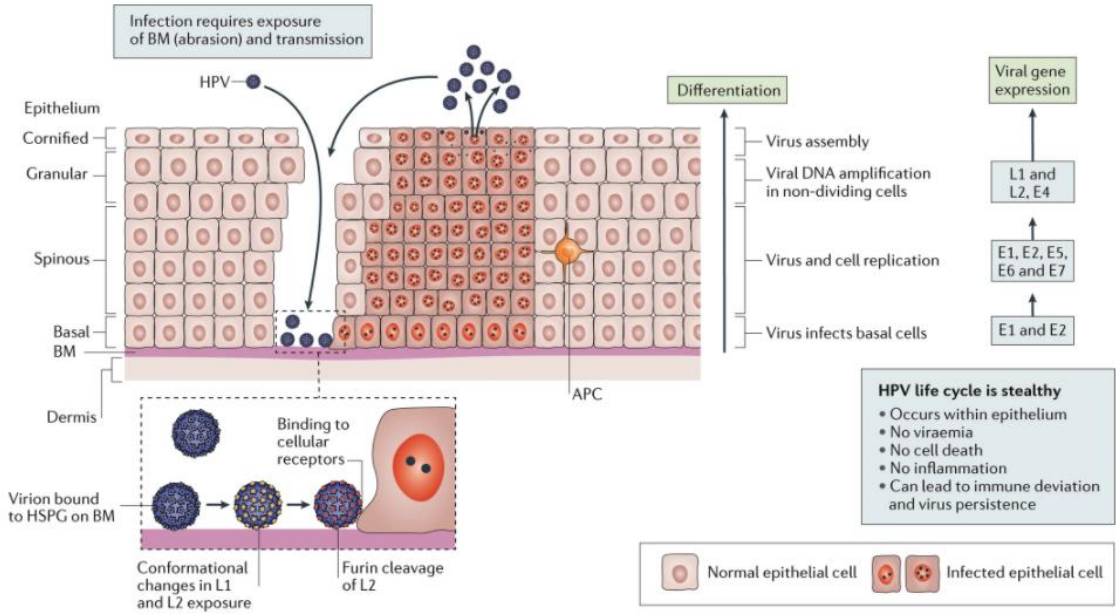

Figure 2. HPV life cycle (Roden and Stern 2018).

The epithelial abrasion exposes the basement membrane and gives virus access to the basal keratinocytes. In the infected cells, the viral genome integrates into the host genome. The E6 and E7 early viral proteins are the major actors, which stimulate the continued proliferation of HPV, and facilitate the environment for E1 and E2 to conduct abundant viral genome replication until achieving a high number of copies. Terminal

differentiation of infected cells happens in the upper epithelial layers. This process activates the E4 expression and then L1 and L2 proteins are expressed in the uppermost layer of the epithelium that leads to packaging of a very high numbers of the viral genome. Maturation of virions occurs after terminal differentiation and HPVs are released as E4 disintegrates the cytokeratin filaments, and the keratinocyte residues are thrown out of the epithelial surface completing the viral life cycle (Figure 2). No apparent inflammation is detected, which avoids the alert of local immune responses (Roden and Stern 2018).

1.1.5 HPV E6 and E7 – Oncoproteins

Cervical cancer is related to the formation and evolution of a persistent infection that is dependent on two important HPV oncoproteins, E6 and E7, which are essential for oncogenic cell transformation. These oncoproteins are responsible for adjusting keratinocyte differentiation and stimulating cell propagation and continuity. The capacity of both proteins to obstruct the cell cycle proliferation system is associated with both low and high-risk classifications of diverse existing HPV types (Almeida et al. 2018).

E7 and E6 oncogenes are expressed by the inactivation of E2 protein expression, which is the transcriptional repressor of E6 and E7. During the genome linearization, the E2 sequence is interrupted since the viral genome is integrated into the host's chromosomal DNA. E6 induces the degradation of the p53 tumor suppressor via cellular ubiquitination, leading to telomerase activation that results in disruption of the cell cycle control, affecting the evolution and extended cell life. E7 can establish complexes with the retinoblastoma (pRb) tumor suppressor, by repressing regulation of replication-associated genes and leading to the transition of the cell life cycle to the S-phase and subsequent host cell genome replication (Pal and Kundu 2019; Chabeda et al. 2018).

The E7 phosphoprotein is relatively small with around 100 amino acids and is constituted with three conserved regions (CR1/2/3). The CR2 domain is composed of a poorly conserved sequence and contains LXCXE motif, which is important for the association with its targets. The CR3 region at the carboxyl-terminal end encodes a zinc finger structure consisting of two CXXC motifs. The pRbs are known as “pocket proteins” and E7 binds pRb in this region named as “pocket domain”. This interaction results in the pRb phosphorylation and degradation. One of the most important functions of pRb is to bind E2F-family transcription factors and repress the expressions of replication enzyme genes. The main protein regulation mechanism that E7 interferes with is between pRb/E2F system. E7 disrupts the interaction between Rb and E2F, resulting in

the release of E2F transcription factors and the subsequent activation of genes promoting cell proliferation (Pal and Kundu 2019; Yim and Park 2005). The mechanism is represented in Figure 3.

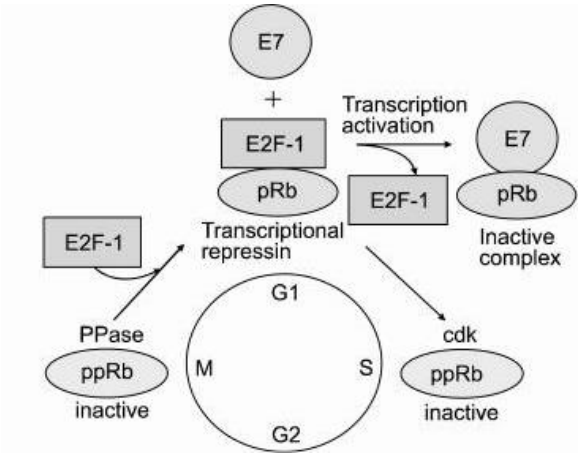

Figure 3. Schematic flowchart illustration of E7 oncoprotein activity (adapted from (Yim and Park 2005)).

The HPV E6 is an oncoprotein larger than E7, with around 160 amino acids. It is organized into two zinc finger binding domains by four Cys-X-X-Cys motifs (structure responsible for the protein oncogenicity). The carboxy-terminal domain, which contains the PDZ-binding motif, allows the interaction with cell proteins containing the LXXLL motif. In the specific case of cervical cancer, this interaction happens with the E6 associated protein (E6AP). HPV E6 bind to the LXXLL sequence in the conserved domain of E6AP, through E3 ubiquitin ligase that works as a connecting bridge between E6 and p53, forming a trimeric complex of E6/E6AP/p53, finally leading to p53 degradation (Pal and Kundu 2019; Yim and Park 2005). The step-by-step process is described in Figure 4.

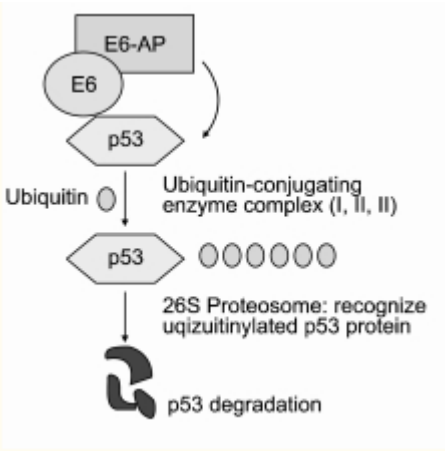

Figure 4. Schematic flowchart depiction of E6 oncoprotein activity leading to p53 degradation (adapted from (Yim and Park 2005)).

1.1.6 Current prevention methods

Quadrivalent HPV vaccine Gardasil®, from Merck (Merck & Co., Kenilworth, NJ, USA), is a prophylactic vaccine against HPV infection. This vaccine is the first commercially available HPV vaccine, licensed by the United States Food and Drug Administration (FDA), in 2006. In 2007, the bivalent HPV vaccine Cervarix® (GSK, Brentford, UK) was approved by the European Medicines Agency (EMA) and by FDA in 2009. Both vaccines prevent the infection from HPV-16 and 18, the most common and carcinogenic virus genotypes, which are responsible for around 70% of cervical cancers (Cheng, Wang, and Du 2020). Gardasil also prevents HPV 6 and 11, which are responsible for approximately 90% of genital warts. The two vaccines are prepared using virus-like particles (VLPs) which consist of L1 proteins. The dominant component of the capsid is the L1 protein and its expression results in the self-assembly of virus-like particles (VLPs). These VLPs have a similar size and shape to HPV virions, however, do not have viral DNA (Cheng, Wang, and Du 2020; Padmanabhan et al. 2010).

In 2014 Merck completely innovated the vaccination market and released a nine-valent vaccine, Gardasil 9, (Merck & Co., Kenilworth, NJ, USA). The new five protections are associated with another 20% of cervical cancer, this way, the new prevention method offers protection against approximately 90% of cervical cancers. By spreading the vaccination among the worldwide population is expected that the cancers related to HPV infections decrease (Cheng, Wang, and Du 2020; Padmanabhan et al. 2010).

However, the current vaccines do not have a therapeutic effect against the already infected cells. This means that the vaccine can only prevent the infection by the HPV, but cannot prevent the cancer development of cancers from pre-existing infections (Almeida et al. 2019). The challenge of developing new approaches against HPV-related cancers made the therapeutic cancer vaccines still a major area of ongoing research.

1.2 DNA-based therapy

DNA is a crucial molecule in all living organisms owing to its coding functions within the cell, providing the necessary information for protein synthesis as well as for the regulation of cellular mechanisms. With advances in biotechnology, DNA recombinant technology was born and continues to grow. The possibility of rearranging different genes and manipulating their functions has led scientists to dedicate their research to the development of new gene-based therapies such as gene therapy and DNA vaccination (Sung and Kim 2019; Ramamoorth and Narvekar 2015).

Gene therapy is defined as the process to treat or enhance the health condition of the patient by inserting therapeutic genetic material (nucleic acids) into somatic cells instead of using drugs or surgery to suppress, modify, or correct/complement the effect of a deficient gene responsible for a disease. It is well known that the mutation of a single or set of genes leads to almost all human health disorders (Sung and Kim 2019)

Gene therapy is divided into two major categories: germline gene therapy and somatic gene therapy. Germline gene therapy consists of the introduction of a gene into reproductive cells (sperm or ovule) or later in the zygote, which results in the transmission of the gene of interest to the offspring. This technique is forbidden due to ethical issues and is not currently applied. Somatic gene therapy consists of the introduction of the gene of interest only into the patient's target cells where the therapy is needed and is not transmitted to future generations (Nayerossadat, Maedeh, and Ali 2012).

1.3 DNA vaccines

Vaccination is considered the greatest contribution to global public health interventions of the latest centuries. The evolution and consequent contribution of vaccines are responsible for an expressive increase in general life expectancy and have resulted in the complete extinction of pathogens that cause many diseases, such as smallpox caused by variola virus and rinderpest caused by rinderpest virus. The most common vaccine approach is protein-based, which requires direct application of weaken/dead viruses or bacteria, recombinant proteins, or VLPs. Beyond this approach present some safety concerns, it only induces an antibody-mediated immune response, which cannot be totally efficient when the pathogens reproduce intracellularly (Walters et al. 2015; Kim, Lee, and Jang 2012).

One of the promising approaches for therapeutic vaccines is DNA vaccination. DNA vaccination is applicable against a great range of viral, bacterial, and parasitic diseases, including HPV (Almeida et al. 2019; Ha et al. 2005; Okuda et al. 2001). In comparison with traditional vaccines, DNA vaccines have numerous promising advantages. They are simpler to synthesize when compared to recombinant protein vaccines and can be produced on a large scale. In general, they are considered to be safer, since the pathogen is not required in the vaccine production. Additionally, DNA vaccines present high stability, which can discharge the need for refrigeration, storage, and transport, allowing

easier distribution worldwide. DNA vaccines are particularly appropriate for antitumor and anticancer treatment since their encoded antigen can be expressed by antigen-presenting cells (APCs) (Almeida et al. 2019; Smith and Klinman 2001; Kutzler and Weiner 2008).

1.3.1 Antigen presentation

DNA vaccination is based on the delivery of DNA vectors, such as the bacterial plasmid DNA (pDNA), encoding one or many immunogenic proteins (antigens) of the same virus or similar proteins which can belong to multiple different contagious agents. The possibility of using multigenic vaccines allows a global immunization, reducing the vaccination numbers that must be performed (Gulce-Iz and Saglam-Metiner 2019).

The process starts once the DNA vaccine reaches/transfects the target cell, where the encoded gene will be transcribed, processed, and expressed by the APC and non-APC cells, being able to stimulate both cellular and humoral immune responses. These cells can then activate the needed immune response for the dissolution or destruction of a recognized infected cell. The expressed antigens will be presented by both major histocompatibility complex MHC class I (intracellular route) and II (extracellular route). The administration of a single dose of DNA vaccine can provide a broad range of the immune response, thereby enabling stimulation of both $CD4^+$ and $CD8^+$ T cells, which secrete cytokines and have a regulatory function in the production of antibodies (Almeida et al. 2019; Anderson and Schneider 2007; Lee et al. 2018; Xu, Yuen, and Lam 2014). There are two major pathways to understand the whole process (Figure 5).

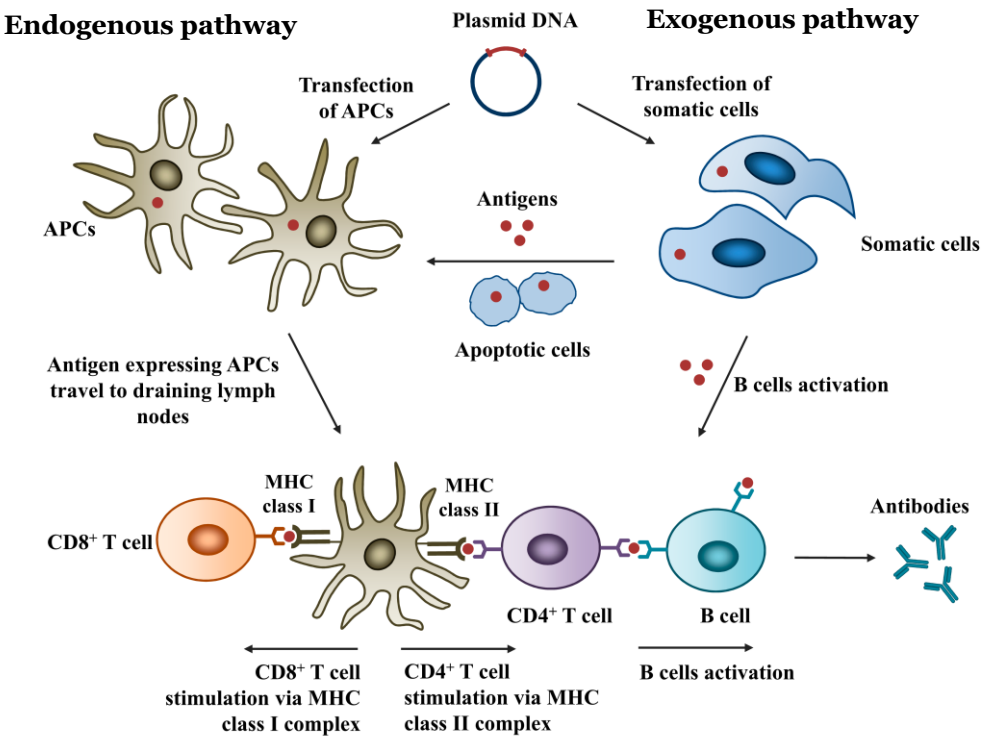

Figure 5. Schematic representation of the antigen presentation – endogenous and exogenous pathways (adapted from (Xu, Yuen, and Lam 2014)).

As presented in figure 5, the intracellular pathway starts when APCs are transfected with pDNA vaccine which will produce the target antigen. This antigen will be presented by MHC class I to simple $CD8^+$ (cytotoxic) T lymphocytes cells, activating them as cytotoxic T Lymphocyte (CTLs). The extracellular pathway starts when APCs catch exogenous antigens, produced by other cells (somatic cells), which were also transfected with the DNA vaccine and expressed the target antigen. Antigens presented through the extracellular route activate MHC class II restricted $CD4^+$ (helper) T cells. Then, these cells, mediate the induction of B cell responses, produce antigen-specific antibodies. The release of a specific antibody may neutralize the pathogen that is in charge of the production of the target antigen (Almeida et al. 2019; Anderson and Schneider 2007; Lee et al. 2018; Xu, Yuen, and Lam 2014).

1.3.2 DNA vaccine delivery routes

Currently, four DNA vaccines have been licensed for animal usage. One against West Nile virus in equine, another against infectious hematopoietic necrosis virus in salmons, third one for melanoma treatment in dogs, which represents the success of DNA vaccines against cancer, and the last one approved for growth hormone-releasing hormone (GHRH) in pigs (Gómez and Oñate 2019).

All these vaccines use intramuscular injection of naked pDNA, which is one of the main routes for DNA vaccine administration. This administration route requires large amounts of the DNA to be administered and external stimulation to encourage the internalization of the DNA. Significant levels of antigen-specific immunity were shown with naked DNA vaccination, however, the intramuscular approach leads to weak immune responses (Farris et al. 2016).

There are many vaccine delivery routes available nowadays that have been considered for DNA vaccines, including parenteral routes (e.g. intramuscular, intradermal, and subcutaneous injection) and mucosal routes (e.g. oral, intranasal, and vaginal) (Farris et al. 2016; Porter and Raviprakash 2017). The main advantages and disadvantages of the routes are described in table 2.

Table 2. Advantages and disadvantages of DNA vaccine delivery routes (adapted from (Farris et al. 2016; Porter and Raviprakash 2017))

Route	Advantages	Disadvantages
Intramuscular	Easy technique; Large volume possible	Invasive; Possible systemic administration; Muscle or nerve damage
Subcutaneous	Easy technique; Large volume possible; Less chance of systemic administration	Fat absorption
Intradermal	Access to the APCs (Langerhans)	Smaller volume (less than 250 uL); More complex technique
Intranasal	Non-invasive; Induction of mucous immune response; Minimum antigen dilution	Possibility of wrong absorption site
Oral	Non-invasive, induction of mucous immune response	Antigen dilution; Greater tolerance
Transdermal	Non-invasive; Easy administration; Easy observation	Allergy; More absorption time

Naked DNA	Safe and simple method; Long-term expression; Able to transfer a gene (2–19 kb)	Efficiency for gene delivery is low; Only proper for some applications such as DNA vaccines

The intranasal vaccine has been widely investigated in recent years. It is a promising pathway because can it offer immune protection against many diseases, including cancer. In addition to the advantages listed in the table 2, this approach also leads to the rapid onset of action and avoidance of first-pass metabolism. The non-invasive administration also gives the opportunity for self-administration avoiding the risk of spreading blood-borne infections because it does not require a needle. Most of the conventional available vaccines are administered by intramuscular, subcutaneous, or intradermal injection, targeting the systemic immune system, however, they are ineffective in inducing local immunity at mucosal sites. Furthermore, the vaccines which are delivered directly to the mucosal site can provide a better and more efficient mucosal immune response. Aiming these advantages, some barriers need to be overcome to allow the successful development of intranasal DNA vaccines (Xu, Yuen, and Lam 2014).

1.4 Gene delivery systems

To get a successful design of a gene delivery system, which can protect and deliver the genetic material in an appropriate manner, three elements need to be understood. Firstly, the plasmid-based gene expression system that regulates the gene action inside the targeting cell; second, the gene itself, which will encode a particular therapeutic protein; and, third, the vector, which will be used as a gene delivery system controlling the delivery of the gene expression plasmid to a particular part of the body. One of the most critical steps regarding the gene therapy application is the vector that will be chosen for delivery. All gene therapy approaches depend on the facility that the genetic material needs to be delivered across the cell membrane and ultimately to the targeted cell nucleus. Since the genetic material alone will be very difficult to be internalized by the cells and can easily be degraded by nucleases, the chosen DNA vectors should be safe and present good transfection efficiency (Sung and Kim 2019; Nayerossadat, Maedeh, and Ali 2012; Ramamoorth and Narvekar 2015).

Vectors emerge as vehicles that can be used in both, gene therapy and DNA vaccines. These vectors transport and deliver the genetic material into a broad variety of cells, tissues, and whole organs. The optimal vector has to make the DNA entrance into the

eukaryotic cell nucleus, if possible, without degradation of the active ingredient incorporated in them, and the gene delivery must happen only to the specific cells (targeted delivery). Additionally, they should be easy to prepare, economic, have low toxicity, and be safe. There are two major classes of vectors, the viral and non-viral vectors, which can be used for gene delivery and they present some advantages and disadvantages (Nayerossadat, Maedeh, and Ali 2012; Ramamoorth and Narvekar 2015; Ibraheem, Elaissari, and Fessi 2014).

1.4.1 Viral vectors

Viruses use their easy invasion capability into eukaryotic cells to inject their DNA inside host cells and take advantage of the host's nuclear machinery. The viruses' ability to replicate and intercalate their genetic materials, and consequently lead to the expression of the target proteins in these cells make them an effective form of gene delivery, moreover, the virus structure prevents degradation via the DNA liposomes. These features made the viruses the first vector option used in gene therapy (Sung and Kim 2019).

The most used viruses for gene delivery systems are retrovirus, adenovirus, adeno-associated viruses, lentivirus, and herpes virus, poxvirus, human foamy virus, and lentivirus. These viruses were chosen due to the high transduction and transcription capacity of the exogenous material inserted in the viral genome (Sung and Kim 2019).

All viral vector genomes have been modified, namely, genes responsible for their pathogenicity are replaced by therapeutic genes or some areas of their genomes are deleted. These adjustments remove the pathogenic effect so that they become incapable of replication. However, they retain the ability to transfect the targeted cells, which is demanding for this type of vector (Nayerossadat, Maedeh, and Ali 2012). In table 3 the advantages, disadvantages, features, genome, and host range of the main viral vectors are depicted.

Table 3. Advantages, disadvantages, features, genome, and host range of viral vectors (adapted from (Ibraheem, Elaissari, and Fessi 2014; Lundstrom and Boulikas 2003)).

Vector	Features	Advantages	Disadvantages
Adeno-associated virus (AAV)	Slow expression onset; Genome integration; Long-term expression; Genome: double-stranded (dsDNA); Host Range: broad.	Integration on human chromosome 19 (wild-type only) to establish latent infection; Prolonged expression; Transduction does not require cell division; Small genome, no viral genes.	Not well characterized; No targeting; Requires packaging cell line; Potential insertional mutagenesis; Limited insert size: 5 kb.
Adenovirus	Transient expression; Strong immunogenicity; Genome: dsDNA; Host Range: broad.	High transduction efficiency *ex vivo* and *in vivo*; Transduces many cell types; Transduces proliferating and nonproliferating cells; Production is easy at high titers.	Remains episomal; Transient expression; Requires packaging cell line; Immune-related toxicity with repeated administration; Potential replication competence; No targeting; Limited insert size: 4-5 kb
Herpes	Latent infection; Long-term expression; Genome: dsDNA; Host range: broad.	Large insert size: 40-50 kb; Neuronal tropism; Latency expression; Efficient transduction in vivo; Replicative vectors available	Cytotoxic; No targeting; Requires packaging cell line; Transient expression does not integrate into the genome
Retrovirus	Long-term expression; Genome integration; Genome: dsDNA; Host range: restricted.	Integration into the cellular genome; Broad cell tropism; Prolonged stable expression;	Inefficient transduction; Insertional mutagenesis; Requires cell division for transfection; Requires packaging cell line; No targeting;

		Requires cell division for transduction; Larger insert size: 9-12 kb	Potential replication competence.
Lentivirus	Long-term expression; Genome integration; Genome: dsDNA; Host range: broad.	Transduces proliferating and nonproliferating cells; Transduce hematopoietic stem cells; Prolonged expression.	Safety concerns: from human immunodeficiency virus origin; Difficult to manufacture and store limited insert size: 8 kb; Limited clinical experience.

This system also presents several weaknesses, such as triggering severe immune and inflammatory responses leading to a degeneration of transducted tissue, potential oncogenic effects with toxin production, and storage instability. In addition, their limitation in transgenic capacity size due to the size of the target DNA sequence is limited and reduced, requiring changes that lead to its preparation, being time-consuming and expensive (Nayerossadat, Maedeh, and Ali 2012; Ibraheem, Elaissari, and Fessi 2014). Consequently, to overcome these drawbacks the non-viral vectors emerge as a promising alternative.

1.4.2 Non-viral vectors

Non-viral systems consist of physical and chemical systems and came up to overcome the obstacles of the viral systems. Although non-viral vectors are less efficient in cell transfection compared to viruses. They present higher cell viability, safer, less immunogenicity, no limitation in size of transgenic DNA, higher biocompatibility, easier production, lower cost and reproducibility as advantages over the other system (Nayerossadat, Maedeh, and Ali 2012). The plasmid DNA is one of the best candidates to carry the gene into the nucleus of the desired cells due to its ability to integrate exogenous DNA and replicate itself inside the nucleus of target cells. Plasmid DNA has been widely investigated because it provides many advantages that fit the features of this kind of vector. The production by bacterial fermentation makes the manufacturing easier to be controlled and also reduces the cost of production. The pDNA needs to be delivered inside the cell nucleus and to overcome the barriers found in cell membranes two methodologies, physical or chemical, can be applied to help the pDNA to go through these limitations. (Ibraheem, Elaissari, and Fessi 2014).

1.4.2.1 Physical methods

The non-viral gene delivery physical method consists of introducing genetic materials through the cell membranes by physical forces (mechanical, ultrasonic, electric, hydrodynamic, or laser-based energy) that weaken the membrane to make it more permeable allowing DNA to easier reach the nucleus. Needle injection, ballistic DNA injection (gene gun), sono-poration, photo-poration, magneto-fection, hydro-poration, and ultrasound are some techniques for this application. Despite these techniques are easy to apply and present high efficiency, they can lead to tissue damage. In table 4 the principles and goals of the main approaches are summarized (Sung and Kim 2019; Nayerossadat, Maedeh, and Ali 2012).

Table 4. Summary description of the different physical methods applied in gene delivery (adapted from (Sung and Kim 2019; Nayerossadat, Maedeh, and Ali 2012)).

Physical Methods	Principles	Goal
Electroporation	Electric pulse that creates pores in a cell membrane	Allow entry of genetic materials
Photo-poration	Laser pulse that creates pores in a cell membrane	Allow entry of genetic materials
Magneto-fection	Magnetic particles are complexed with DNA and an external magnetic field	Concentrate nucleic acid particles into target cells
Hydro-poration	Hydrodynamic capillary effect	Manipulates cell permeability
Gene Gun	Spherical particles are coated with plasmid DNA and accelerated to high speed by pressurized gas	Penetrate into target tissue cells
Ultrasound	Nanomeric pores in the membrane	Facilitate intracellular delivery of DNA particles into cells of internal organs or tumors, so the size and concentration of plasmid DNA have a great role in the efficiency of the system.

1.4.2.2 Chemical methods

Chemical vectors are more commonly used than physical methods. In this last approach, the DNA is conducted through the membrane until the nucleus by carriers, which are prepared by chemical reactions leading to DNA encapsulation. The nanocarriers

produced by chemical systems can be synthetic or natural (Ibraheem, Elaissari, and Fessi 2014).

The two most important non – viral vectors for gene delivery are cationic phospholipids and cationic polymers. These cationic materials can be easily and efficiently combined with negatively loaded DNA by electrostatic interactions, creating nanomeric complexes called lipoplexes or polyplexes, respectively. These nanomeric complexes are generally stable enough to protect their bound nucleic acids from degradation and are competent to enter cells usually by endocytosis (Nayerossadat, Maedeh, and Ali 2012).

Polymer-based non-viral vectors use polymers to interact with DNA and form polyplexes. Polyplexes when compared with lipid-based nanoparticles present some advantages such as lower cytotoxicity, easier manipulation, higher stability, and more controlled release of target DNA (Valente et al. 2021). The polymer-based vectors are categorized into two groups: natural and synthetic polymers. Natural polymers are proteins, peptides, and polysaccharides the synthetics are Polyethyleneimine (PEI), dendrimers, and polyphosphoesters (Ramamoorth and Narvekar 2015).

Non-viral systems must permit the delivery of genetic material to target cells. The chemical systems allow the encapsulation of the nucleic acid inside vectors with a positive external charge. Since the cell membrane has a negative charge, these vectors enable the genetic material to overcome cellular barriers delivering DNA more efficiently compared to physical systems (J. W. Wang and Roden 2013). Three main characteristics such as DNA condensation, protection from nucleases, and delivery of genetic material only to target cells make the non-viral vectors a very promising alternative to viral carriers (Ibraheem, Elaissari, and Fessi 2014).

1.5 Nanocarrier systems

Nanocarriers have gained huge attention in nanomedicine due to their efficient drug delivery in several target cells, considering different applications, since diagnosis, prevention, or therapy of innumerous pathologies. They exhibit some fascinating properties regarding limited steric obstruction, due to the nanometer size and the ability to protect the therapeutic cargo, not only at the extracellular but also at the intracellular level (Panyam and Labhasetwar 2003). Particles with uniform shape, ranging in size between one and one thousand nm and containing neutral or positive surface charge, are considered ideal to carry drugs and efficiently deliver them into eukaryotic cells. The

successful application of nanoparticle (NPs) is also determined by several desirable features, including their capacity to penetrate through several anatomical barriers, sustained and controlled release of their contents locally, their stability, and biocompatibility (Patra et al. 2018).

Nanoparticles are known to have a high surface/volume proportion and, the active ingredient or biopharmaceutical can be annexed to their surface or also combined in their core or matrix (Figure 6) (Christoforidis et al. 2012; Li and Huang 2008).

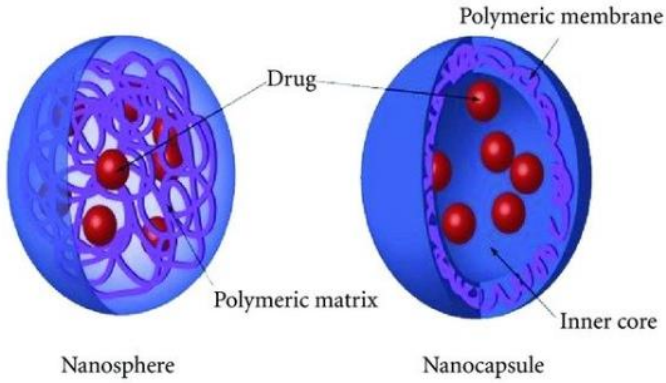

Figure 6. Different types of polymeric nanoparticles. Nanosphere (matrix system) and nanocapsule (repository system) – Source: Nanomedicine (2010) Future Medicine Ltd. (Adapted from (Christoforidis et al. 2012)).

Regarding the movement of drugs within the body, nanocarriers, in most cases offer many advantages, such as reduced clearance, extended circulation time, increased biological half-life, the possibility of surface modification for target delivery, and additionally increase the mean residence time (MRT) in the circulation system (Li and Huang 2008). Several materials, such as liposomes, dendrimers, peptides, and polymers (synthetic or natural origin), have been explored in the formulation of nanocarriers to improve drug delivery and scale down toxicity (Patra et al. 2018; Geszke-Moritz and Moritz 2016; Saad et al. 2008; Chauhan 2018; Pudlarz and Szemraj 2018).

1.5.1 Liposomes

Liposomes were first identified by Bangham and co-workers in the 1960s and characterized as swollen phospholipid systems. The first approach of liposomes application was for parenteral delivery. Later on, they tried to use them in oral delivery at the beginning of the 1970s, they showed intensely low oral bioavailability. Liposomes can consist of natural or synthetic lipids, but their components are not restricted to lipids, and can be produced from polymers. In that case nanoparticles are called

polymersomes. All the compositions of liposomes, synthetic or natural lipids or polymers, make them biocompatible and biodegradable allowing them for biotechnology and biomedical studies. Liposomes are basically made of two parts an aqueous core surrounded by a lipid bilayer. This lipid layer acts comparable to a membrane, isolating the inside aqueous core from the bulk outside (Fan and Zhang 2013; Torchilin 2005).

However, liposomes constituted of lipids show very low physical stability in the gastrointestinal tract (GIT) and for labile compounds as biomacromolecules they are far from being the optimal carrier system. Generally, there are widespread concerns with the physical stability of liposomes in the GIT. For labile biomacromolecules, liposomes are not ideal carrier systems in order to their instability and the fast degradation of leaked cargo consequent to disruption of the liposomal structure. This situation can be different for insoluble drugs in water. In these circumstances, the fragments of liposomes can form new mixed micelles. In these cases, the encapsulated drugs are moved to the new transport mechanisms and carried to the intestinal epithelium for absorption (Jumaa and Müller 2000; Tian et al. 2016).

Liposomes have a very common drawback regarding digestion/penetration, that is their instability The instability begins when liposomes are ingested and exposed to the rough habitat of the GIT. Ordinary liposomes, formed by phospholipids and cholesterol, are very vulnerable to physiological aspects such as gastric acid, bile salts, and pancreatic lipases. The lipases hydrolyze the liposomal phospholipids disrupting their structure compromising their integrity and hence leakage of the payload. Researches show that liposomes can lose integrity in approximately 2 h in simulated intestinal fluid with seriously damaged structure. Bile salts, a surfactant secreted by the liver, can disrupt the liposomal structure composed of lipids with lower phase transition temperatures (Wu, Lu, and Qi 2015; W. Liu et al. 2015).

1.5.2 Solid Lipid Nanoparticles

The solid lipid nanoparticles (SLNs) are nano or micro-sized colloidal carriers, which are composed of physiological lipid, dispersed in water or an aqueous surfactant solution. SLNs are composed of a solid lipid core with one layer of phospholipid shell and they generally have a spherical morphology that can be investigated with TEM (Transmission electron microscopy) and SEM (scanning electron microscopy). They are used as a substitute carrier system to traditional colloids, such as liposomes and emulsions. The phospholipids have a hydrophobic (lipophilic) and hydrophilic (lipophobic) structure

and the lipophilic subdivision of phospholipids is inserted in the lipid matrix (Figure 7). Many drugs or medicines can be involved by SLNs, principally hydrophobic ingredients (Geszke-Moritz and Moritz 2016; Lin et al. 2017).

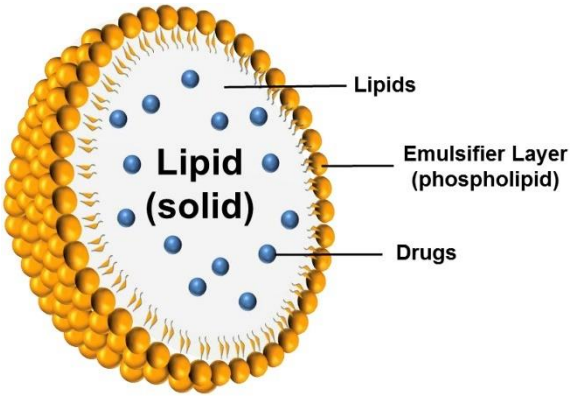

Figure 7. Solid Lipid Nanoparticles structure (Lin et al. 2017).

SLNs offer benefits such as biocompatibility and stability against coalescence. Some labile compounds are protected by the nanoparticle matrix because of their solid state. This fact can also prolong drug release and also present chemical versatility. The nontoxicity is another advantage of the SLNs and low cytotoxicity to animal cells, showing tolerable results to the body. SLNs can be orally administered, dispersed in the aqueous phase or at different dosage forms like capsules, tablets, pastille, and pellets (Lin et al. 2017; Ezzati Nazhad Dolatabadi, Valizadeh, and Hamishehkar 2015).

In comparison to the liposome approach, the SLNs have more drug stability and prolonged release However, there are many disadvantages of SLNs, such as lipid particle growth, the gelation that cannot be predicted, restricted transdermal drug delivery, loss of high amounts of drugs, lack of controlled drug release, and the low percentage of incorporation associated with their crystalline architecture (Das and Chaudhury 2011; Sinha et al. 2011).

1.5.3 CS nanoparticles

Among the diversity of nanoparticle applications in biomedicine, the complexation of nucleic acids for gene therapy or vaccine delivery has been considered an emergent approach (Baden et al. 2021). Among polyplexes, CS appears as one of the most frequently mentioned polymers in the life sciences research studies, handling an extensive range of biopharmaceutical and biomedical approaches and applications (Bellich et al. 2016).

CS is a natural linear polycationic polymer, composed of D-glucosamine and N-acetyl-D-glucosamine combined by β (1→4) linked glucosamine residues, being considered one of the best alternatives to constitute polymeric nanoparticles. Chitin is easily found in nature, the biopolymer is from the insects' and crustaceans' shells and is also present in cell walls of fungi and bacterias (Badazhkova et al. 2020). This polysaccharide (CS) shows good biological features for therapeutic application in comparison to other materials, such as good biocompatibility, biodegradability, adsorption, and poor toxicity. Several studies also describe CS carriers as suitable non-viral vectors for gene delivery, considering the biological properties mentioned above and its cationic character, which favors nucleic acids encapsulation via electrostatic interaction and cellular internalization as shown in the schematic representation in Figure 8 (Raik et al. 2018; Agirre et al. 2014; C.-K. Chen et al. 2020). CS properties, such as molecular weight, deacetylation degree (DDA), CS derivatives, N/P ratio, suitable crosslinker, must be taken into consideration while choosing the best alternative of optimal CS for efficient and effective gene delivery (Cao et al. 2019).

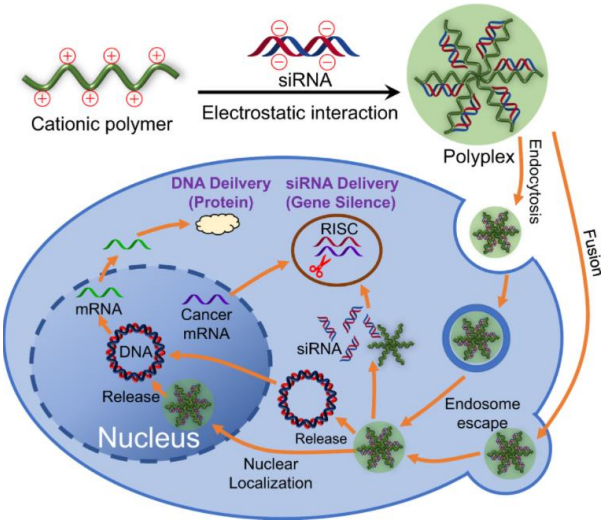

Figure 8. Schematic of gene delivery system of polyplexes (C.-K. Chen et al. 2020).

1.5.3.1 CS mucoadhesion property

CS is a natural, biodegradable polysaccharide polymer that has many applications because it can easily and quickly be functionalized to produce several products with distinct functional properties. In addition, CS is bioadhesive (mucoadhesive) which improve the entrance of molecules through the mucosal surface (Badawy and Rabea 2011). The mucoadhesive property of CS particles prolongs the residence time of the NPs in the mucosal areas, offering advantages for mucosal drug delivery, such as more

effective absorption, easier application and controlled release of loaded pharmaceutics. (Ensign, Cone, and Hanes 2012).

Mucus is a viscoelastic, adhesive hydrogel layer produced from goblet cells, mucus secretory cells, or submucosal glands. It covers all exposed epithelial surfaces not covered by skin, such as the surface of lung airways, GIT, female reproductive tracts, eye, nose, and other mucosa. Mucus protects the underlying epithelium by lubricating the surface and most foreign particulates and pathogens are efficiently trapped and removed in mucus layers via steric obstruction and adhesion. Mucus forms adhesive interactions with pathogens, environmental fine particles, and conventional particle-based drug delivery systems, which can be hydrophobic forces, electrostatic interactions, hydrogen bonds, or Van der Walls interactions. The mucus turnover is the mechanism that promotes their removal and lasts minutes to hours (Ensign et al. 2012).

The predominant constituent of mucus is water, approximately 95% by weight. The composition of mucus goes from cross-linked and tangled mucin fibers, swamped cells, bacteria, lipids, salts, proteins, macromolecules, and cellular debris. Depending on the mucosal surface, the mucus pH and thickness can considerably change. In a very acid environment, which means low pH, the mucin fibers must aggregate and the mucus viscoelasticity will increase. In the intestine, the digestive action and the food consumed can vary the mucus thickness (Netsomboon and Bernkop-Schnürch 2016).

In addition, mucus accomplishes an important role in human health. Mucus layer is structured by deeply crosslinked mucin fibers, developing a thick compressed porous design, which contains highly glycosylated (negative charged) segments. These mucin fibers contain hydrophobic areas, which can wrap hydrophobic particles. These interactions have great advantages, such as avoiding the transport of many malicious agents, bacteria, for instance (Ensign et al. 2012; Netsomboon and Bernkop-Schnürch 2016; M. Liu et al. 2015).

The adherence between two materials is called mucoadhesion, when at least one of these materials is the mucosal membrane. The particles that are mucoadhesive tend to get trapped in the mucus layer, are unable to penetrate across the mucus layer and to go through the underlying epithelia. Mucoadhesive particles (MAPs) are related to the mucus layer via interactions with mucin fibers (Figure 9). For example, particles with positive charges in their surface interact with the mucin and are trapped by them. The

alteration time of the mucoadhesion system is related to the physiological turnover time of the mucus layer. The ordinary nanoparticles generally do not adhere to the mucosal surface for more than five hours. To overtake this problem, various types of polymers have been studied as mucoadhesive agents in particulate drug delivery systems. These different kinds of polymers can extend/prolong the mucosal residence time of active molecules at the site of application/absorption and, afterward, enhance drug delivery to mucosal membranes (Ensign et al. 2012; Netsomboon and Bernkop-Schnürch 2016; M. Liu et al. 2015; Lai, Wang, and Hanes 2009).

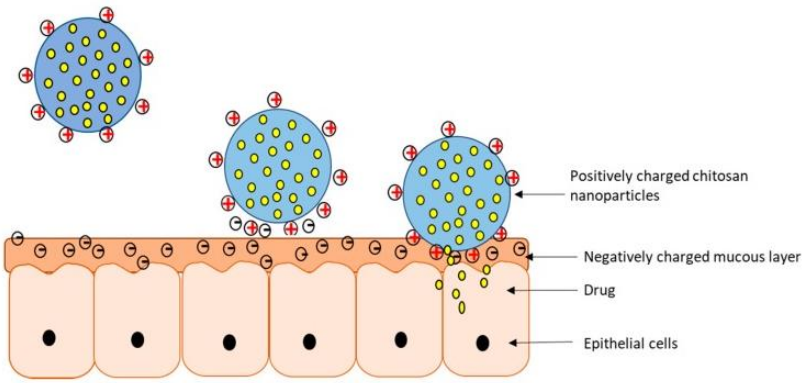

Figure 9. Schematic representation of mucoadhesion system between positively charged CS loaded nanoparticles with the mucus layer (adapted from (Mohammed et al. 2017)).

1.5.3.2 Methods for CS nanoparticles preparation

CS has been mentioned to be more effective to improve drug uptake when developed in the nanoparticulate form in comparison to solutions. There are many diverse routes to prepare CS-based nanoparticles and several methods have been designed and reported with different applications to reach the desired requirements. The most general methods are ionotropic gelation, microemulsion, emulsification solvent diffusion, and emulsion-based solvent evaporation (Table 5) (Mohammed et al. 2017; Chandra Hembram et al. 2016).

Table 5. Methods for preparation of CS nanoparticles (adapted from (Mohammed et al. 2017; Chandra Hembram et al. 2016)).

Method	Technique	Advantages	Disadvantages
Complex coacervation method	Nanoparticles are formed by coacervation of the positively charged amino groups of CS and the negatively charged DNA phosphate groups.	The process can be entirely performed in an aqueous solution at a low temperature; The method is simple, there is an absence of harsh	Poor stability of the NPs; Low drug loading and crosslinking of the complex by a chemical reagent.

		conditions and the nanoparticles form spontaneously	
Coprecipitation	It involves coprecipitation of CS solution, prepared in low pH acetic acid solution, to high pH 8.5 – 9.0 solution such as ammonium hydroxide resulting in the formation of highly monodisperse nanoparticles.	Very small particles; High encapsulation efficiency; Uniform distribution of nanoparticles	A wide range of particle size is seen with this method
Micro-emulsion	Nanoparticles are formed in the aqueous core of reverse micelle by adding surfactant. The solution is kept on continuous stirring allowing the nanoparticles to form overnight as the cross-linking process is completed	Very narrow size distribution; Size can be controlled by the concentration of glutaraldehyde in the preparation of the NPs; Small-sized nanoparticles	Usage of organic solvent - Organic solvent is then removed by evaporating under low pressure; Long/Tedious process; Complex washing step;
Emulsification solvent diffusion	An o/w emulsion is prepared by mixing organic solvent into a solution of CS with a stabilizer under mechanical stirring followed by high-pressure homogenization. nanoparticles are formed upon polymer precipitation	High encapsulation efficiency of hydrophobic drugs	Need for harsh preparation conditions, such as organic solvents and high shear forces
Solvent evaporation	Addition of CS to the aqueous phase forming emulsion and precipitation by ultrasonication. The emulsion solution is added to a surfactant and stirred until evaporation of the organic solvent, resulting in NPs.	Nanoparticles in a range of 50 and 300 nm can be reached	Multiple washing and centrifugation steps are required to get rid off excess surfactant

Reverse Micellar	The surfactant is dissolved in an organic solvent followed by the addition of CS, drug, and crosslinking agent, under constant overnight vortex mixing. The organic solvent is evaporated resulting in the formation of transparent dry mass.	Ultrafine nanoparticles of around 100 nm or even less.	The difficult isolation of nanoparticles; The need for larger amounts of solvent.
Ionotropic gelation	This process derives from inter-and intramolecular cross-linkages mediated by the anionic molecules. Nanoparticles are readily formed due to complexation between positive and negative charged species during mechanical stirring at room temperature	The processing conditions are mild and it uses a hydrophilic environment; Low toxicity; Little chance of altering the chemistry of the drug to be encapsulated.	Poor stability in acidic conditions.

Ionotropic gelation is the most used method that allows the formation of nanoparticles and microparticles. They are formed by electrostatic interactions between the CS solution (positively charged) dissolved in acid solutions (acetic acid, acetate buffer) and a cross-linking, any polyanionic solution (negatively charged). A high number of polyanions have been used, but to avoid the possible toxicity of reagents and other undesirable effects, tripolyphosphate (TPP) is the most used anionic crosslinker to produce the gelation of CS. CS does not dissolve in the presence of water. However, using diluted acids, the protonation of the amine groups in the polymer molecules occurs, and CS solubility increases. This phenom makes the electrostatic interactions with negatively charged species possible (Figure 10) (Chandra Hembram et al. 2016; Subhashis Debnath, R. Suresh Kumar 2011; Pedroso-Santana and Fleitas-Salazar 2020).

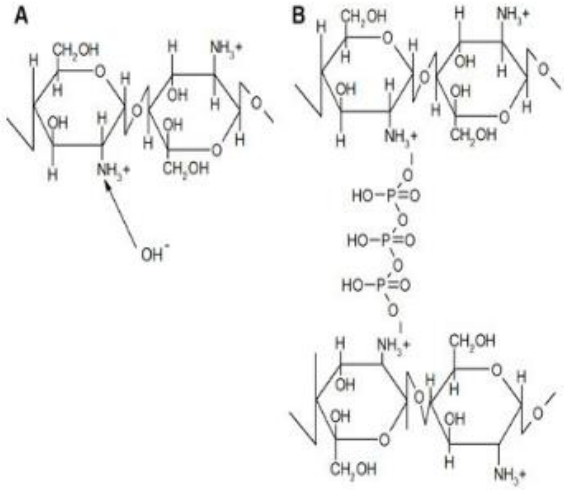

Figure 10. Chemical schematic of CS/TPP combination **(A)** Deprotonation, **(B)** Ionic crosslinking (Chandra Hembram et al. 2016).

This kind of technique permits a controlled release of the drug and offers other advantages, such as co-encapsulation of molecules, specific activity place with functionalization of the particles, and extra time of the drug's bioactivity. In addition, ionotropic gelation is very economic and simple. This methodology requires less equipment and time and, the fact of using reversible physical cross-linking instead of chemical cross-linking improved cell viability and drug integrity (Chandra Hembram et al. 2016; Subhashis Debnath, R. Suresh Kumar 2011; Pedroso-Santana and Fleitas-Salazar 2020).

2 Objective

The goal of this thesis consisted of the design and development of a polyplex CS-TPP-pDNA delivery system, which will encode the E7 protein. After reaching the best formulation of the nanocarrier the present work had to achieve a successful gene expression and consequently, protein expression and, therefore, therapeutic effect against cervical cancer. To achieve this effort, an efficient delivery system has been formulated, containing a set of appropriate features (morphology, size, encapsulation efficiency, surface charge, stability, protection effect, biodegradability, non-toxic, reproducibility) to pDNA vaccine delivery.

Therefore, this work consisted of using the ultra-pure CS polymer to encapsulate the plasmid DNA that encodes the E7 gene by the ionotropic gelation technique. The properties of the nanoparticles were studied using different parameters to achieve the best formulation system. The nanocarrier system with the best conditions will be evaluated according to the desired gene delivery application. Finally, *in vitro* biological activity evaluations were performed on Fibroblasts and Raw cells to test cellular viability, uptake, and internalization as well as their transfection efficiency and the investigation of its potential cancer therapeutic effect as an alternative to conventional therapies applied in the current clinical environment.

3 Materials and Methods

3.1 Materials

Medical grade CS 95/1000 was purchased from Heppe Medical, sodium tripolyphosphate (TPP) was obtained from Across Organics, deoxyribonucleic acid sodium salt (DNA) was acquired from MPBIO, 35% hydrochloric acid (HCl), sodium hydroxide palettes (NaOH), and glacial acetic acid were all acquired from VWR. The following solutions were freshly prepared by using deionized water from VWR: 2M HCl, 10M NaOH, 1%, and 2% (v/v) acetic acid. GRS Taq DNA polymerase was purchased from Sigma Aldrich Chemicals (St. Louis, MO, USA). $MgCl_2$ was obtained from NZYTech, Lda. TripleXtractor used in RNA extraction was obtained from GRISP (Porto, Portugal). DMEM-F12 and DMEM-HG were purchased from GIBCO (Waltham, Massachusetts, USA). Sodium bicarbonate was obtained from MP Biomedicals (Santa Ana, USA). Agarose and GreenSafe were obtained from NZYtech (Lisbon, Portugal). All solutions were freshly prepared by using ultra-pure grade water, purified with a Milli-Q system from Millipore (Billerica, MA, USA).

3.2 Methods

3.2.1 Production of the plasmid DNA – E7

The pMC.CMV-MCS-EF1-GFP-SV40PolyA pDNA vaccine, encoding human papillomavirus E7 protein next to CMV promoter (Figure 11), was amplified in the *Escherichia coli* host. At first, the bacterial strains were inoculated in Luria-Bertani (LB)-agar plates containing 50 μg/mL of the kanamycin antibiotic and incubated overnight at 37°C to grow. This step intends to help the cell recovery from the cryopreservation and adapt to the nutrients of the solid medium by direct contact in a small surface area. After the growth step in the solid medium, some colonies were recovered and transferred to a 250mL Erlenmeyer containing 62.5mL of Terrific Broth (TB) liquid pre-fermentation medium made up of 20 g/L of tryptone, 24 g/L of yeast extract, 4mL/L of glycerol, 0.017 M of KH_2PO_4, 0.072 M of K_2HPO_4 in 7.0 pH, supplemented with 50 μg/mL kanamycin. This step is called pre-fermentation and aims second adaptation of the cells to a little volume of liquid medium. The volume of the pre-fermentation medium used was ¼ of the total capacity of the Erlenmeyer to guarantee the correct oxygenation of the cells. The

cells were put to grow at 37°C in a shaking orbital (Agitorb Aralab® 200, Albarraque, Portugal) at 250rpm. The optic density (OD) was measured until the desired number of 2.6 (corresponding to the exponential cell growth). After reaching approximately this OD, a specific volume of this medium containing cells was calculated as in equation (1), where Vp.i. is the pre-inoculum volume, Vf is the fermentation volume, ODd is the fermentation desired optic density and ODp.i. is pre-inoculum OD and transferred to four 500mL capacity Erlenmeyers with 125mL of TB fermentation medium.

$$(1)\ Vp.i. = \frac{(Vp.i. + Vf) * \mathrm{ODd}}{ODp.i.}$$

The solutions were incubated at 37 °C overnight for approximately 18 h at 250 rpm, after this period, bacterial growth was interrupted, and the final fermentation solution divided into 50 mL Falcon tubes in order to recover the cells by centrifugation at 4500 rpm for 10 minutes at 4 °C and the pellets were stored at -20 °C until further use.

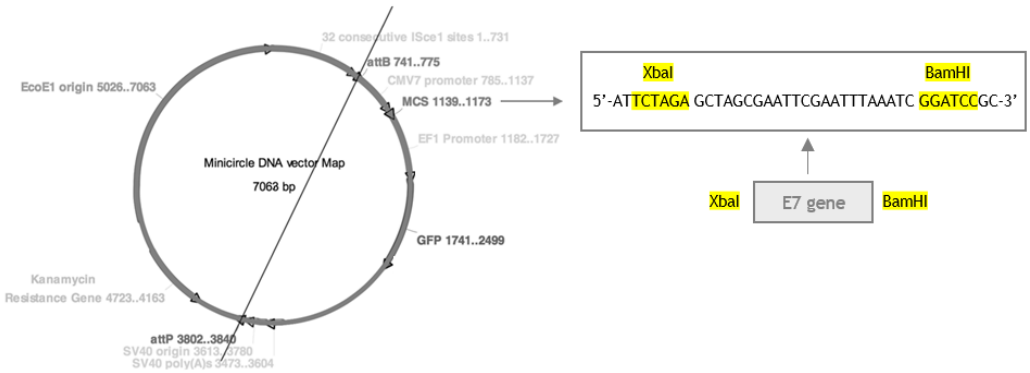

Figure 11. Schematic representation of the E7 gene cloning in the plasmid DNA.

3.2.2 Extraction and purification of pDNA

After the fermentation process, NZYTech Plasmid Maxi kit was used to obtain the plasmid extraction, recovery and purification, following the manufacturer's recommendations. The frozen pellet from the fermentation was taken and put to thaw into ice, after thawing the pellets, 20 mL of P1 solution was added to the pellet to keep the cells in isotonic conditions, shaking vigorously the solution into the vortex to resuspend the pellet. After that, the content was divided into two lysis tubes, 10mL in each, and 10mL of P2 solution was added. Tubes were shaken gently (5x) to avoid the degradation of the plasmid and incubated for 5 minutes at room temperature to perform the cell lysis. Then, to stop the process of lysis, 10 mL of P3 solution was added to each tube. Tubes were inverted gently 5x to homogenize the solution, then they were incubated for 20 minutes into the ice. Tubes were centrifuged twice at 20.000 RCF for

30 minutes at 4°C, changing the supernatant into another clean lysis tube between centrifugations. This centrifuging step is important to get rid of contaminants, such as cell debris, gDNA, unwanted proteins. The anion exchange resin was used, starting by the equilibrium step with 10 mL of QBT buffer solution, respecting the manufacturer's instructions. Supernatants of lysis tubes were added to the column. Afterward, 30 mL of QC solution (washing solution) was added to the column twice and all the liquid with unwanted proteins and low molecular weight molecules was discarded. For the next step, another clean lysis tube was taken and put into ice under the column, and 15mL of QF solution (elution solution) was added to the column to recover the pDNA. Cold isopropanol at the ratio of 0.7 x QF solution (15 x 0.7 = 10.5mL) was used to precipitate the pDNA and the solution was homogenized very gently using the roller agitator for 10 minutes inside the cold chamber. The obtained sample was incubated for 20 minutes into the ice. The sample was centrifuged 16.000 RCF for 30 minutes at 4°C. The supernatant was discarded and the pellet dried at room temperature. The pellet was resuspended in 1 mL buffer of 10mM Tris-HCl at pH of 8.0 and stored at -80°C. The final concentration of the sample was quantified using the Nanophotometer equipment.

P1 Solution – 50mM of Tris-HCl pH of 8.0, 10mM of Tris-EDTA, 100µg/mL of RNAse A

P2 Solution – 200mM of NaOH, SDS 1% (w/v)

P3 Solution – 3.0M of potassium acetate pH of 5.0 and SDS 1% (w/v)

QBT – Balance solution – 750mM NaCl, 50mM MOPS, 15% Isopropanol (v/v), 0.15% Triton X-100(v/v), pH of 7.0

QC – Washing solution – 800mM of NaCl, 50mM of MOPS, 15% of Isopropanol, pH of 7.0

QF - Elution solution – 1.75mM of NaCl, 50Mm of Tris, 15% Isopropanol, pH of 8.5

3.2.3 Electrophoresis

Agarose gel was prepared in the concentration of 1%, 0.4 g of Agarose diluted in 40 mL of TAE 1x buffer (40 mM Tris base, 20 mM acetic acid, 1 mM EDTA at pH 8.0), with the addition of 0.6 µL of green safe. The liquid solution was put into a form to solidify for 40 minutes. After the solidification, the gel was taken and put into a vat. An amount of 18 µL of each sample was added inside the well with 2 µL of loading buffer. The loading buffer is composed of water, glycerol, and bromophenol blue with the purpose of well deposition of samples and helping to visualize the run migration. The electrodes were adjusted to 120 V and run for 40 minutes. The gel analyses were made through Uvitec Fire-Reader system (UVITEC, United Kingdom).

3.2.4 Ionotropic Gelation

The method used to prepare the CS-TPP-pDNA polyplexes was the ionotropic gelation, using CS as a polymer and TPP as a crosslinker. Particles with and without DNA and pDNA were prepared following the process adopted from (Nunes et al. 2021; K.-Y. Chen and Zeng 2018; Özbaş-Turan and Akbuğa 2011) with some adjustments. Particles without DNA and pDNA were used as a negative control. The process of ionic gelation is depicted in Figure 12. The CS stock solution was prepared in the concentration of 0.1% (w/v) in 1% (v/v) acetic acid, and the TPP stock solution was prepared in the concentration of 0.1% (w/v) in deionized water. The pH of CS and TPP stock solutions was adjusted to 5.2–5.5 and 2 by the addition of NaOH and HCl, respectively. Several dilutions of stock solutions were considered as well as different volumes of each solution to explore the best conditions for the nanoparticle formulation. Then, both CS and TPP solutions were filtered using a 0.20 μm polyethersulfone syringe filter (from VWR). For the experiments with synthetic DNA and pDNA encapsulation, both samples were dissolved into the TPP solution to reach the concentration of 35 μg/mL and 20 μg/mL, respectively. A syringe pump (Harvard Apparatus 11 Plus, USA) was used to add TPP/TPP-DNA/TPP-pDNA solution to the CS solution dropwise with a flow rate of 0.25 mL/min. To accomplish regular drop size, a needle size of 20 G was used in all experiments, leading to an addition rate of about 15–16 drops/min. During the addition, the CS solution was stirred vigorously (600 rpm) using a magnetic stirrer. After the complete addition of TPP/TPP-DNA, the final solution was mixed for 30 min. As a positive control, 0.1% (w/v) of synthetic DNA in water was prepared and mixed with the blank particles without DNA in 1:1 ratio (by volume). The combined solution was incubated for 2h at room temperature for DNA adsorption to CS-TPP nanoparticles to take place. All experiments were accomplished at room temperature, in triplicates and the results are presented as means ± standard deviation (S.D.).

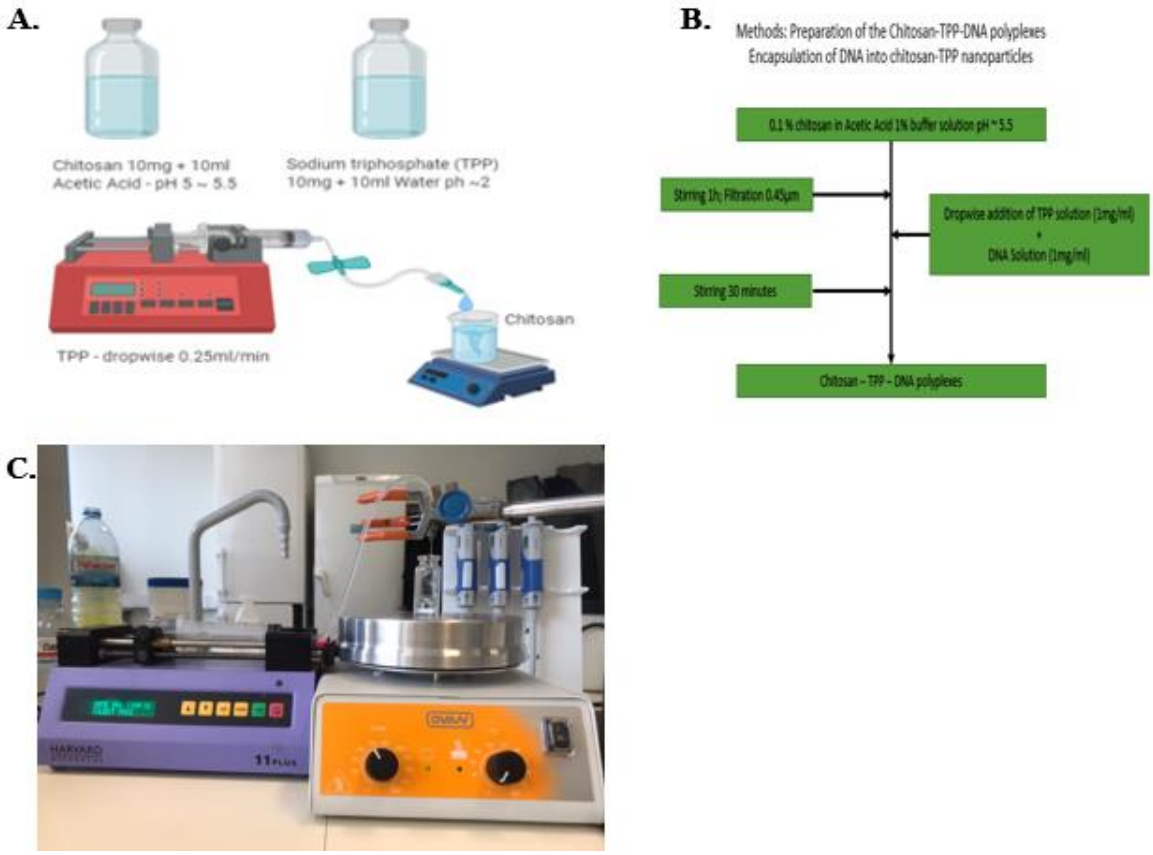

Figure 12. (A) Schematic illustration of CS-TPP nanoparticles **(B)** Flow chart of the nanoparticle with DNA preparation. First solutions with optimized concentrations were prepared. Then TPP with DNA was added to CS solution dropwise while stirring **(C)** Laboratory assembly for ionotropic gelation method

3.2.5 Encapsulation Efficiency

To estimate the amount of the DNA encapsulated in the CS NPs, the NPs solution was spun down using Centrifuge Hettich Mikro 200 (Tuttlinggen, Germany) for 10 minutes at different speed rates to reach the best formulation, and the DNA concentration in the supernatant was measured using the NanoPhotometer™ at 260 nm. The indirect encapsulation efficiency (iEE) was calculated as in equation (2), where c(total) is the theoretical DNA concentration in the solution and c(sup) is the measured DNA concentration after the encapsulation.

$$(2)\ iE.E.\% = \frac{c(total) - c(\mathrm{sup})}{c(total)} * 100\%$$

To verify the accuracy of the method, the amount of the encapsulated DNA was also estimated in the particles by the direct encapsulation efficiency (dEE). NPs with and without DNA were spun down for 20 minutes at 22000 RCF. The supernatant was removed for iEE measurement and the equivalent volume (1 mL) of 2% acetic acid and an additional 100 µL of 2 M HCl were added to the pellet for nanoparticle degradation and release of encapsulated DNA to measure dEE. The solution was vortex for one

minute and then sonicated using the ultrasound homogenizer (from Qsonica sonicators) for 30 seconds at 40% amplitude. The dEE was calculated as a ratio of measured and theoretical DNA concentrations. In both cases, DNA concentration was determined spectrophotometrically, by adding the supernatant or dissolved nanoparticle solution (1 mL) to the quartz cuvette. The solution was diluted 2 to 3 times with 1% acetic acid, and the absorbance was measured using a cuvette reader from SpectraMax. The absorbance value at 260 nm was recorded.

3.2.6 Particle size determination

The size and charge of the prepared CS-TPP-pDNA polyplexes were also analyzed, using the Zetasizer Nano ZS analyzer (Malvern Instruments, Worcestershire, UK), equipped with a He-Ne laser by Dynamic Light Scattering (DLS). The particles were analyzed immediately after the preparation (0h), 72 h, and after one month to evaluate the stability of the particle suspension. All DLS experiments were carried out at a temperature of 25 °C in triplicate and recorded into Zetasizer software v 7.03 (Malvern Instruments, Worcestershire, UK).

3.2.7 Scanning Electron Microscopy (SEM)

The geometry and morphology of CS-TPP-pDNA nanoparticles were evaluated by Scanning Electron Microscopy (SEM). Freshly prepared systems with pDNA encapsulated were centrifuged (10 000 rpm, 10 min, 4 °C), the supernatant was discarded and the pellet resuspended in phosphate-buffered saline (PBS) solution, another centrifugation was performed in same conditions, and the pellet suspended in an aqueous solution containing 40 µL of 2 % tungsten. The samples were diluted 1:10 in ultra-pure grade water. From the diluted solution, 10 µL was pipetted to roundly shaped coverslip (10 mm) and let dry overnight at room temperature. On the next day, samples were assembled on aluminum holders, attached with double-sided adhesive tape, and sputter-coated with gold using an Emitech K550 (London, England) sputter coater. A scanning electron microscope, Hitachi S-2700 (Tokyo, Japan) with an accelerating voltage of 20 kV, various magnifications were used to evaluate the morphology of nanoparticles.

3.2.8 Stability assay

First, 250 µL of particles were centrifuged at 10 000 RCF for 10 minutes at 4 °C, then the supernatant was removed and analyzed by electrophoresis 1% agarose gel for 40 minutes and 120 V to evaluate the presence of pDNA in the supernatant of the systems without DMEM-F12 medium and trypsin. The pellet was resuspended in 25 µL of DMEM-F12

medium supplemented with 10% of FBS and incubated for 0, 2 and 6 h at 37 °C, the same systems were equally centrifuged, but resuspended with 25 µL of trypsin and incubated for 0, 2 and 6 h at 37 °C. The samples were applied in the electrophoresis 1% agarose gel for 40 minutes 120 V to evaluate the degradation and release of the particles. Three controls were done, pDNA alone, with DMEM-F12 medium and with trypsin, respectively.

3.2.9 Cell culture experiments

The experiments were performed in two different cell lines, cell culture experiments were performed using Human Fibroblast cells (ATCC® PCS-201-012™) and Raw 264.7 cells (murine macrophage cells, ATCC® TIB-71™). The fibroblasts cells were grown in Dulbecco´s Modified Eagle´s Medium with Ham's F-12 Nutrient Mixture (DMEM-F12) supplemented with 10% v/v heat activated FBS, 2.438 g/L sodium bicarbonate, and 1% (v/v) of a mixture of antibiotics composed of penicillin (100 µg/mL) and streptomycin (100 µg/mL). Raw cells were grown Dulbecco´s Modified Eagle´s Medium with High Glucose (DMEM-HG) supplemented with 10% not inactivated fetal bovine serum, 1.5 g/L sodium bicarbonate and with 1% (v/v) the same mixture of antibiotics was used as described above. The cells were seeded in 25 cm^2 T-flasks at 37 °C in 5% CO_2 humidified environment until the cell confluence (50-60%). For fibroblasts, the medium was removed and 1 mL of 0.18% trypsin 1:250 with 5mM EDTA was added to unfold the cells and the T-Flask was incubated at 37°C for 5 minutes. After the incubation 2 mL of complete DMEM-F12 medium (double volume of trypsin) was added to stop the action of the trypsin the 3 mL mixture was added to a 15 mL Falcon tube and centrifuged at 300 RCF for 5 minutes, the supernatant was discarded and the pellet resuspended in 1 mL of complete medium for the cell recovery. For Raw cells, the medium was discarded and the cells were recovered adding 2 mL of complete medium and the T flask scratched with a cell scraper. For transfection studies, Human fibroblast cells and Raw cells were seeded in 12-well plates at a density of 2.5×10^5 cells/well and 2×10^5 cells/well, respectively, in 1 mL complete medium. After 24 h and before transfection occurs, the medium was replaced by a medium without FBS and antibiotic supplementation (incomplete medium), in order to promote transfection. When the intended confluence was reached, the medium was removed and the cells were transfected with particles dissolved in the incomplete medium. After 6 h of transfection, the incomplete medium was replaced by the complete medium.

3.2.10 *In vitro* Transfection Studies

3.2.10.1 Cell viability assay

The cell viability was evaluated by the resazurin assay. For the experiment hFIB and Raw cells were seeded in a density of $1x10^4$, for both, per well in a 96 well-plate. After 24 h of seeding the cells, the complete medium was changed to a simple medium (without FBS and antibiotic) after 12h of changing the medium the cells were transfected with the NPs, 6h after the transfection the simple medium was changed again to complete medium. After 24h of the transfection the medium was discarded and a mixture of 100 µL of complete medium + 20 µL of resazurin to each well. The plate was incubated in the dark for 4h at 37°C in 5% CO_2 humidified. The volume of 100 µL of the mixture was transferred to each well of an opaque plate, the fluorescence excitation at 544 nm and emission at 590 nm were read. The measures were performed using a plate reader spectrofluorometer (Spectramax Gemini XS, Molecular Devices, San Francisco, CA, USA). The same procedure was repeated after 48h of transfection. The relative cell viability (%) related to control wells was calculated by [A]sample / [A]control × 100, where [A]sample is the absorbance of the tested sample and [A]control is the absorbance of the control sample. Two controls were done, negative control with non-transfected cells and positive control where Ethanol 70% was added to promote the apoptosis of the cells. All the experiments were repeated three times in triplicate.

3.2.10.2 RNA extraction

The RNA extraction was done in two different cell lines, hFIB and Raw cells were seeded in a density of $2.5x10^5$, per well in a 12-well-plate. To extract total RNA, the medium inside the wells was removed and the well was washed twice with PBS to remove all the liquid. The cells were lysed through the addition of 200 µL of TripleXtractor (GRISP, Porto, Portugal) to each well, homogenization was performed with the pipette by doing "up and down" with the liquid inside the well until a viscous solution be noticed, a new tip was used to each homogenization process. The samples were incubated for 5 minutes at room temperature. Chloroform was added in the amount of 50 µL to each sample to perform the separation of the different biomolecules, the samples were vigorously mixed by inversion. The samples were incubated for 10 minutes at room temperature and then were centrifuged at 4 °C for 15 minutes at 12000 RCF. After the centrifugation, two different layers were noticed. The top layer containing the aqueous phase was gently recovered in order to avoid the destabilization and contamination of the RNA. The precipitation of RNA was performed using 125 µL of cold isopropanol and the samples were carefully mixed by inversion. The samples were incubated on ice for more 10

minutes and centrifuged at 4 °C for 15 min at 12000 RCF. The supernatant was removed and the pellet was resuspended in 125 µL 75% ethanol (prepared in diethylpyrocarbonate (DEPC) water) to eliminate the organic compounds, then the samples were centrifuged at 4 °C for 5 min at 12000 RCF. The supernatant was discarded, and, the pellet was dried for 5 minutes and rehydrated with 20 µL of DEPC water. The RNA was quantified at the NanoPhotometer™.

3.2.10.3 cDNA synthesis

The synthesis of the cDNA was done with Xpert cDNA Synthesis kit (GRiSP Research Solutions, Porto). A mixture of 1 µg of RNA sample described above, 1 µL of Deoxynucleotide (dNTPs), 1 µL of random primers and RNase free water until reach the final volume of 14.5 µL was prepared in a RNase free tube. The tubes were incubated at 65 °C for 5 minutes and after put into ice for 2 minutes. Thereafter, 4 µL of buffer, 0.5 µL of RNase Inhibitor and 1 µL of Xpert RTase were added to the prepared mix and was gently homogenized. The samples were incubated in three different time duration at 3 different temperatures. They were put into the T100™ Thermal Cycler (Bio-Rad Laboratories, Inc, Hercules, California, USA), at 25°C for 10 minutes, 50 °C for 50 minutes, and finally at 85°C for 5 min. After the cDNA synthesis, samples were used to perform the RT-PCR assay or stored at -20°C until further use.

3.2.10.4 Reverse transcription-polymerase chain reaction (RT-PCR)

Qualitative mRNA expression of E7 was evaluated by reverse transcription-polymerase chain reaction (RT-PCR). For PCR experiment, a mixture of 0.7µL of Magnesium chloride ($MgCl_2$), 0.25µL of Deoxynucleotide (dNTPs), 0.40 µL of forward primer (5′–AAT CTA GAA TGC CTG ATA CAC CTA C -3′) and primer reverse (5′ -ATG GAT CCT TAT GGT TTC TGA GAA CAG A -3′), 1.25 µL of buffer, 1 µL of the cDNA sample synthesized as mentioned above, 0.25 µL of GRS Taq DNA polymerase and 8.25 µL of RNase free water. Samples were then put into the T100™ Thermal Cycler (Bio-Rad Laboratories, Inc, Hercules, California, USA), with the subsequent settings: 95 °C for 5 min, 26 cycles of 30 s at 95 °C, 30 s at 60 °C and 1 min at 72 °C, finally 10 min at 72 °C and to finish the amplification, samples were put into 4 °C. The final samples were analyzed by electrophoresis and visualized in UVItec Gel documentation system under UV light (UVItec Limited, Cambridge, United Kingdom).

3.2.10.5 Reverse transcription-quantitative real-time PCR (RT-qPCR)

The level of transcripts was also analyzed quantitatively by RT-qPCR. The mix for a reaction with primers designed for the transcript of the E7 gene was prepared with 10 µL

of SYBR ™ Green Master Mix, 0.64 µL Forward(FW) primer, 0.64 µL Reverse (RV) primer, 7.72 µL of sterile H_2O and 1 µL of cDNA, resulting in a volume of 20 µL per reaction and the mix for a reaction with the primer pair of the GAPDH housekeeping gene transcript (FW: 5'- ATG GGG AAG GTG AAG GTC G -3 '; RV: 5'- GGG GTC ATT GAT GGC AAC AAT A -3') was prepared with 10 µL of NZY qPCR Green Master Mix (2x), 1.2 µL FW primer, 1.2 µL RV primer, 7.5 µL of sterile H_2O and 1 µL of cDNA, reaching a final volume of 20 µL. The reaction mixtures were placed in a Real-Time CFX ConnectTM system (BioRad, United States of America), programmed with the following sequence of incubations: 10 min at 95 °C and 40 cycles of 15 sec at 95 °C, 30 sec at 60 °C.

3.2.11 Statistical analysis

Each experience was performed at least three times. Data are expressed as a mean ± standard error (S.D.). The statistical analysis performed was a one-way and two-way analysis of variance (ANOVA), followed by Tukey and Bonferroni tests. Data analysis was performed in GraphPad Prisma 6 software. A *p*-value below 0.05 was considered statistically significant. Additionally: * $p < 0.05$; ** $p < 0.01$; *** $p < 0.001$; **** $p < 0.0001$.

4 Results and Discussion

Ionotropic gelation is a popular method for DNA encapsulation. Multiple authors have demonstrated the ability to prepare nanoparticles with DNA obtaining sizes below 300 nm (L. Wang et al. 2018; K.-S. Huang, Sheu, and Chao 2009). Wang and co-authors have shown that particles smaller than 200 nm can be prepared by using a solution with low CS and TPP concentrations of 0.1% (L. Wang et al. 2018). In the present work, for the first analysis we have used low solution concentrations of 0.1% and slow controlled drop-wise addition in order to make nanoparticles with a small size. We first investigated the influence of the TPP volume, DNA concentration, flow rate speed of TPP addition, and CS concentration on the size, polydispersity (PDI), charge, and encapsulation efficiency of formed nanoparticles.

4.1 Influence of changing TPP volume

To investigate the influence of the TPP amount solution on nanoparticle size and DNA encapsulation efficiency, four NPs solutions with different volume addition of TPP-DNA into CS solution were prepared. In these experiments, 35 μg/mL DNA was used, 0.1% TPP in four different volumes (1, 1.25, 1.5, and, 2 mL, and 5 mL) and 5 mL of 0.1% CS. As shown in table 6 and Figure 13 **(A)**, using the ionotropic gelation with controlled addition speed, very small nanoparticles of 30-60 nm were obtained. Only the particles with a high TPP amount led to the formation of larger particles of about 57 nm. In all cases, the particle size did not change significantly after storing them at 4°C in the fridge for 72 h. Only a slight increase of about 2-6 nm was detected. However, as shown in Table 6, formed particles were not monodisperse since the PDI index is > 0.5.

Table 6. Average particle size, PDI, and encapsulation efficiency of CS-TPP-DNA polyplexes with different TPP volumes.

TPP volume added (mL)	Z-Average Size (nm)	PDI	Z - Average Size after 72h (nm)	PDI after 72h	Encapsulation efficiency (%)
1.0	45 ± 0.5	0.55 ± 0.01	47 ± 6.9	0.51 ± 0.006	77 ± 10
1.25	37 ± 0.3	0.50 ± 0.03	40 ± 0.9	0.48 ± 0.004	73 ± 5
1.50	39 ± 1.7	0.46 ± 0.04	45 ± 0.9	0.40 ± 0.009	69 ± 4
2.0	57 ± 0.8	0.50 ± 0.02	63 ± 1.9	0.46 ± 0.010	66 ± 4

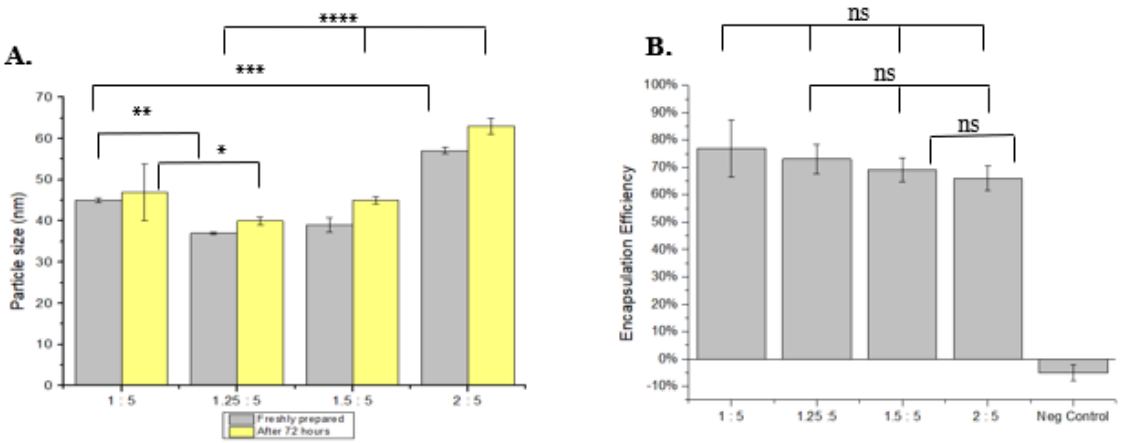

Figure 13. (A) Particle size (nm) freshly prepared and after 72 h with different TPP volumes; **(B)** Results of the encapsulation efficiency with different TPP volumes. Statistical significance was accepted at a level of * $p < 0.05$; ** $p < 0.01$; *** $p < 0.001$; **** $p < 0.0001$, ns - no statistical difference.

Increasing the TPP amount (1.25 mL to 2.0 mL) led to larger particles, clusters, sedimentation and aggregation. The same results were observed by Huang and Lapitsky where primary 20 - 50 nm nanoparticles were obtained and then aggregated into larger and polydisperse particles obtained at the end of the particle formation process. They suggested that bridging flocculation occurs when a flocculant (in this case TPP) simultaneously binds to two particles and causes aggregation by "bridging" the particles together. This bridging has been proposed as the dominant aggregation mechanism during the formation of CS/TPP nanoparticles (Y. Huang and Lapitsky 2017).

The DNA amount encapsulated in nanoparticles was measured using the direct method – after nanoparticle deterioration and release of encapsulated DNA from the collected nanoparticles. Before the measurement, the amount of the DNA that was adsorbed on the surface of the NPs was evaluated, through the positive control, by mixing the prepared NPs without DNA (blank NPs) with the addition of DNA solution (35 µg/mL) after producing the particles and measuring the concentration of the DNA in the supernatant. The obtained results indicated -0.98±1.21 µg/mL of DNA in measured supernatant (data not shown), indicating that very little amount of the DNA may be adsorbed on the NP's surface. As shown in Figure 13 **(B)**, a negative control, blank nanoparticles without any addition of DNA, was done to check the interference of any chemical used for the NPs preparation in the encapsulation efficiency. The negative control showed that there is no interference between the ingredients used in particle preparation. As shown in Figure 13 **(B)**, all formulations showed a good encapsulation efficiency with measured dEE of 77%, 73%, 69%, 66% for samples 1 to 4 respectively. Increasing the TPP-DNA amount led to a decrease in the encapsulation efficiency of about 10%. Since TPP has negative charges and so does the pDNA a competition for the

cationic amino groups of CS happens leading to a decrease in encapsulation efficiency meanwhile the TPP amount increases. The same results were observed by Masarudin and co-authors where CS nanoparticles were formed through the cross-linking of CS chains by TPP via amino group ionic interactions. These results showed that the fraction of free primary amino groups decreased with TPP, indicating a preference/increase in the cross-linking interactions between the cationic amino groups of CS and the anionic TPP to form nanoparticles (Masarudin et al. 2015).

4.2 Influence of changing the DNA concentration

To investigate the influence of the DNA concentration on the nanoparticles size and DNA encapsulation efficiency, four formulations of NPs with DNA concentrations of 15, 25, 35, and 45 μg/mL were prepared. As mentioned before, particle size was measured immediately after the preparation and after 72 h to evaluate the NPs stability. The results are summarized in Table 7 and depicted in Figures 14 **(A)** and **(B)**. In all cases, very small nanoparticles below 40 nm were formed, however, the formed nanocarriers are polydisperse. These results suggest a common drawback of very small CS nanoparticles that were also identified by Masarudin and co-authors. They suggest that conventional nanoparticle synthesis often leads to the formation of large particles or aggregates of smaller particles due to the mucoadhesive nature of CS (Masarudin et al. 2015). The particle size of the formulation with low pDNA amount slightly increased after storage, but in general, the particles can be considered stable.

Table 7. Average particle size, PDI, and encapsulation efficiency of CS-TPP-DNA polyplexes with different DNA concentrations.

DNA Concentration (μg/ml)	Z-Average Size (nm)	PDI	Z - Average Size after 72h (nm)	PDI after 72h	Encapsulation efficiency (%)
15 ± 5	40 ± 0.8	0.59 ± 0.01	50 ± 4.8	0.39 ± 0.26	56 ± 28
25 ± 5	35 ± 0.5	0.48 ± 0.05	35 ± 0.5	0.53 ± 0.006	60 ± 13
35 ± 5	36 ± 0.8	0.47 ± 0.05	35 ± 0.3	0.56 ± 0.006	59 ± 4
45 ± 5	38 ± 0.7	0.47 ± 0.04	36 ± 0.4	0.55 ± 0.01	69 ± 2

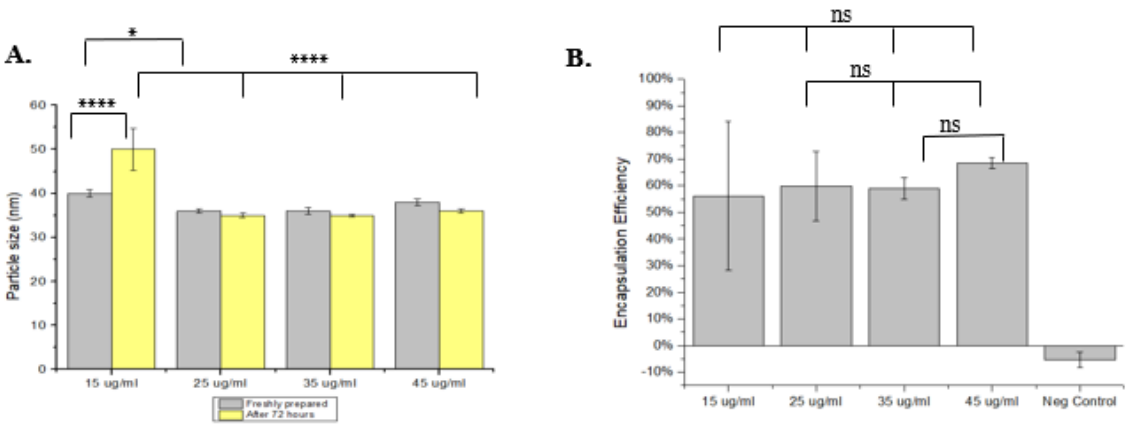

Figure 14. (A) Particle size (nm) freshly prepared and after 72 h with different DNA concentrations; **(B)** Results of the encapsulation efficiency with different DNA concentration. Statistical significance was accepted at a level of * $p < 0.05$; ** $p < 0.01$; *** $p < 0.001$; **** $p < 0.0001$, ns - no statistical difference.

The encapsulation efficiency measurement of nanoparticles with different amounts of TPP-DNA solution added was evaluated as described before. As shown in Figure 14 **(B)**, in all cases good encapsulation efficiencies were reached, dEE of 56%, 60%, 59%, 69%. Overall, our results suggest even with a low concentration of DNA we still have good encapsulation efficiency.

4.3 Influence of changing the flow rate speed of the TPP addition

To analyze the influence of TPP-DNA addition speed on the NPs formulation, four experiments with flow rates of 0.10, 0.25, 0.50, 1.00 mL/min were developed. Solutions with 0.1% TPP, 35 µg/mL DNA and 5 mL of 0.1% CS were prepared. Also, NPs stability was evaluated after 72h. The results are summarized in Table 8 and depicted in Figures 15 **(A)** and **(B)**, showing that the increase of the flow rate speed leads to larger and more polydisperse particles.

Al-Nemrawi and co-workers also analyzed the influence of flow rate of the TPP solution addition but between 0.25 and 2.5 mL/min. According to their results, the same pattern is observed as the TPP solution flow rate increases, the particle size increases, as well as the PDI. They suggested that increasing the rate of addition, higher concentration of TPP at the interface between the CS and TPP solutions happens. The consequence of forming larger particles could be explained by higher inter/intra cross-linkages (Al-nemrawi, Alsharif, and Dave 2018). The particle size did not increase after storage suggesting good stability.

Table 8. Average particle size, PDI, and encapsulation efficiency of CS-TPP-DNA polyplexes with different flow rate speed of TPP addition.

Flow rate (mL/min)	Z-Average Size (nm)	PDI	Z - Average Size after 72h (nm)	PDI after 72h	Encapsulation efficiency (%)
0.10	47 ± 6.5	0.4 ± 0.32	44 ± 1.2	0.48 ± 0.09	65 ± 7.3
0.25	49 ± 2.6	0.50 ± 0.23	50 ± 1.2	0.53 ± 0.05	66 ± 4.1
0.50	72 ± 1.4	0.60 ± 0.08	74 ± 3.9	0.58 ± 0.25	66 ± 4.4
1.00	132 ± 5.6	0.62 ± 0.31	138 ± 1.4	0.65 ± 0.017	62 ± 5.1

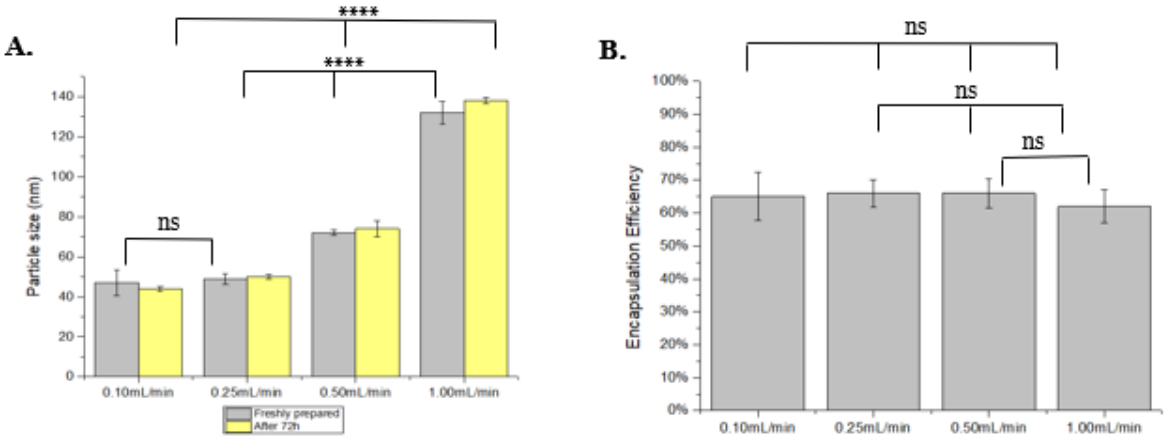

Figure 15. **(A)** Particle size (nm) freshly prepared and after 72 h with different addition flow rates of TPP; **(B)** Results of the encapsulation efficiency with different flow rates addition of TPP. Statistical significance was accepted at a level of * $p < 0.05$; ** $p < 0.01$; *** $p < 0.001$; **** $p < 0.0001$, ns - no statistical difference.

The encapsulation efficiency measurement of nanoparticles with different addition flow rates of TPP solution was evaluated as described before. As shown in Figure 15 **(B)**, in all cases good encapsulation efficiencies were reached, dEE of 65%, 66%, 66%, 62% for the evaluated samples respectively. Overall, our results suggest that no difference in encapsulation efficiency is observed in the different flow rate speeds analyzed.

4.4 Influence of changing the concentration of CS

To analyze the influence of CS concentration on the NPs formulation, four different CS concentrations (0.05, 0.1, 0.25, 0.35 %) were explored and after 72h NPs stability was evaluated. The results are summarized in Table 9 and depicted in Figures 16 **(A)** and **(B)**. We can see that the particle size is directly affected by the CS concentration, the lower the concentration is the smallest are the particles. This is a parameter that we can use to control the size of the particles. Similar results were observed by L. Wang and co-authors, since the increase of the polymer concentration induced an increase in particle

size (L. Wang et al. 2018). The result is also in accordance with Sreekumar and co-authors study, where they found that particles prepared from CS with degree of acetylation of 20% and 50% showed a broad size range from nano to micrometers in hydrodynamic diameter when the CS concentration was increased from 0.5 mg/mL to 5 mg/mL (Sreekumar et al. 2018).

Table 9. Average particle size, PDI, and encapsulation efficiency of CS-TPP-DNA polyplexes with different CS concentration.

CS Concentration (%)	Z-Average Size (nm)	PDI	Z - Average Size after 72h (nm)	PDI after 72h	Encapsulation efficiency (%)
0.05 ± 5	27 ± 0.4	0.51 ± 0.002	29 ± 0.09	0.43 ± 0.02	76 ± 4.5
0.1 ± 5	51 ± 0.6	0.62 ± 0.05	52 ± 1.2	0.53 ± 0.13	70 ± 13.4
0.25 ± 5	75 ± 4	0.62 ± 0.18	81 ± 1.4	0.72 ± 0.008	74 ± 8.4
0.35 ± 5	200 ± 25	0.61 ± 0.03	200 ± 6.4	0.76 ± 0.04	48 ± 7.0

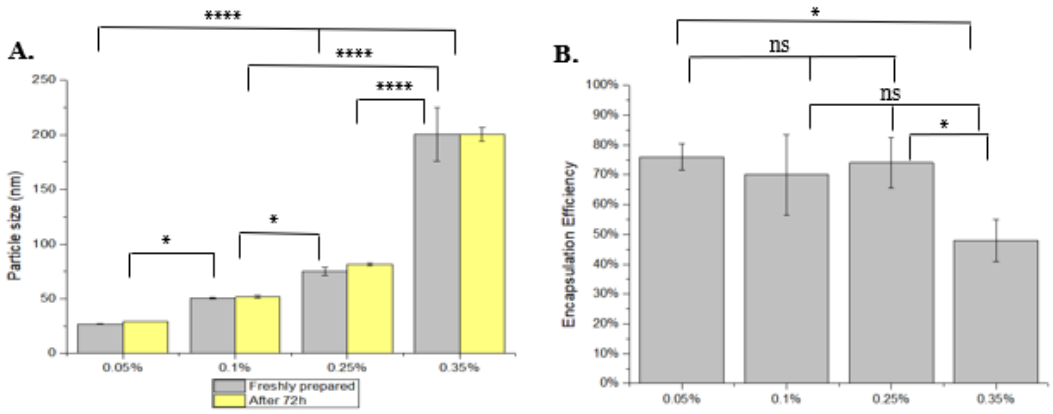

Figure 16. (A) Particle size (nm) freshly prepared and after 72 h with different CS concentrations; **(B)** Results of the encapsulation efficiency with different CS concentrations. Statistical significance was accepted at a level of * $p < 0.05$; ** $p < 0.01$; *** $p < 0.001$; **** $p < 0.0001$, ns - no statistical difference.

In general, all formulations showed good encapsulation efficiency and decreasing the CS concentration is not observed significant alteration in the results. Nonetheless, aggregates were seen in the solution while increasing the CS concentration and were confirmed by forming very polydisperse particles (PDI > 0.6). A similar study was evaluated by Whiteley and co-workers and they found that the PDI was significantly influenced by the interaction between CS concentration and TPP, showing that at lower TPP concentrations PDI increases with increasing CS concentrations (Whiteley et al. 2021).

4.5 Decreasing the PDI of the NPs

Preliminary studies previously described regarding the preparation and formulation of the CS-TPP and CS-TPP-DNA polyplexes shown that very small nanoparticles of 30-50 nm and satisfactory EE were obtained by changing the CS concentration and TPP volume or DNA concentration. However, all formulations showed PDI values above 0.45 (Nunes et al. 2021). The distribution of clusters can be a problem regarding cell internalization, even with small particles. Decreasing the PDI leads to more homogeneous nanoparticles and higher PDI indicates non-uniformity, resulting in broad particle size distribution (Danaei et al. 2018).

The polydispersity on particles was analyzed by Huang and Lapitsky they affirmed that to ensure the formation of monodisperse particles with homogeneous size distributions, both, particle formation and aggregation must occur at the same rate throughout the sample. However, the difficulty to reach this condition is associated with the fact that CS/TPP particles are often produced faster than the required time to mix the parent CS and TPP solutions. This feature leads to significant particle formation/aggregation appearing before TPP is consumed by the sample (Y. Huang and Lapitsky 2017).

Expecting to obtain reasonable results of encapsulation efficiency, cell transfection, gene expression, low cytotoxicity, this issues of high PDI, aggregation and cluster formation needed to be improved, and some other parameters were investigated to reach the ideal formulation system.

4.5.1 Influence of changing TPP volume

Using the ionotropic gelation method Al-Nemrawi and colleagues, obtained particles ranging from 145 to 663 nm. In their study, they proved that by reducing the amount of TPP added a decrease in particle size is observed. In all their formulations, the nanoparticles had positive charges that were reduced at higher TPP concentrations (Al-nemrawi, Alsharif, and Dave 2018). In a study with medium molecular weight (MMW) and high molecular weight (HMW) CS polymers, Zaki and coworkers observed that the CS concentration can directly affect the nanoparticles´ size, i.e., the increase of CS and TPP concentration resulted in an increase of nanoparticles´ size (Omar Zaki, Ibrahim, and Katas 2015). Thus, in the present work, the analysis of changing these two parameters, CS and TPP, exploring the variation of their volume and concentration without DNA presence were done. First, the volume of TPP was changed in three different formulations, presented in the table 10 below. Physico-chemical properties of

these formulations, such as size, PDI and charge, determined by DLS and Zeta Sizer, were recorded and presented in figure 17.

Table 10. Formulations changing TPP volume to reach the best formulation system.

Formulation codes	CS concentration (%)	CS volume (mL)	TPP concentration (%)	TPP volume (µL)
F1	0.035	5	0.1	500
F2	0.035	5	0.1	1000
F3	0.035	5	0.1	2000

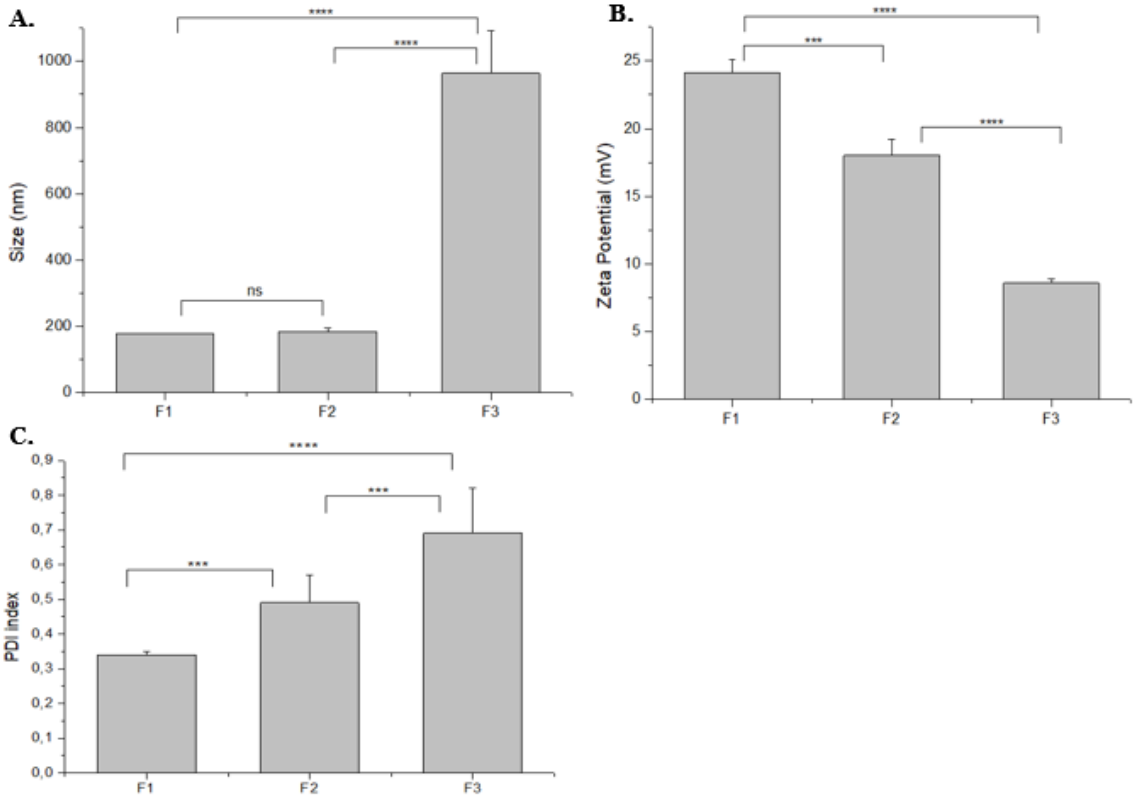

Figure 17. (A) Nanoparticles mean size (nm), **(B)** Average zeta potential, **(C)** Polydispersity index, of the three different TPP volumes analyzed. The values were calculated with the data obtained from three independent measurements (mean ± S.D., n = 3) * $p < 0.05$; ** $p < 0.01$; *** $p < 0.001$; **** $p < 0.0001$, ns - no statistical difference.

Regarding the particle size, results confirmed a small decrease of around 7 nm from sample F1 to F2, by reducing the TPP volume. From sample F3, an increase of the TPP volume to 2 mL showed aggregates/flocculation, which could be proved from the results depicted in figure 17 **(A)** leading to particle size of almost 1000 nm, and was also observed clusters inside the solution. The same effect was evaluated by Tzeyung and co-authors they found that keeping the drug concentration of 0.05%, CS and TPP concentration of 0.05% and varying the TPP volume (5,6, and 7 mL). An increase of 10 nm was observed from 5 to 6 mL, however, increasing the volume to 7 mL a huge difference of 98 nm was noticed (Tzeyung et al. 2019).

Concerning the charge analyzed by zeta potential, sample F1 showed the best result among others, reaching a charge around 24 mV, which is in accordance with the literature. Since TPP is negatively charged and in samples F2 and F3 more TPP volume is added to the solutions, results showed in figure 17 **(B)** confirm that these formulations have less positive charge.

To ensure an improvement on cell uptake, the charge of the NPs should be more positive, since the cell membranes are negatively charged. In this way, the opposite charges benefit the electrostatic attraction between them and improve the internalization. However, after addition and encapsulation of pDNA, the surface charge can be reduced, because DNA is negatively charged. Further studies with pDNA will be evaluated to check this phenom.

From sample F1 and F2, small particles are observed, however, regarding the PDI depicted in figure 17 **(C)**, polydisperse particles are formed, showing high/not satisfactory PDI values. An enormous difference in PDI value can be detected, decreasing the TPP volume, reaching values below 0.35, in formulation F1. Koping-Hoggard and coworkers also observed a decrease in the PDI to 0.25 (Csaba, Köping-Höggård, and Alonso 2009). In this study, the same effect is noticed when comparing samples F1 and F2 where the PDI index decreases 0.15.

4.5.2 Influence of changing CS volume and TPP concentration

Results from the last section showed that the PDI was improved by decreasing the TPP volume to 500 µL, justifying that this parameter will be sustained. Thus, new formulations are described in table 11 by maintaining the TPP volume and now manipulating the CS volume and TPP concentration. Also, physico-chemical properties of these formulations, such as size, PDI and charge, determined by DLS and Zeta Sizer, were recorded and presented in Figure 18.

Table 11. Formulations changing CS volume and TPP concentration to reach the best formulation system

Formulation codes	CS concentration (%)	CS volume (mL)	TPP concentration (%)	TPP volume (µL)
F4	0.035	3	0.1	500
F5	0.035	4	0.1	500
F6	0.035	3	0.05	500
F7	0.035	4	0.05	500

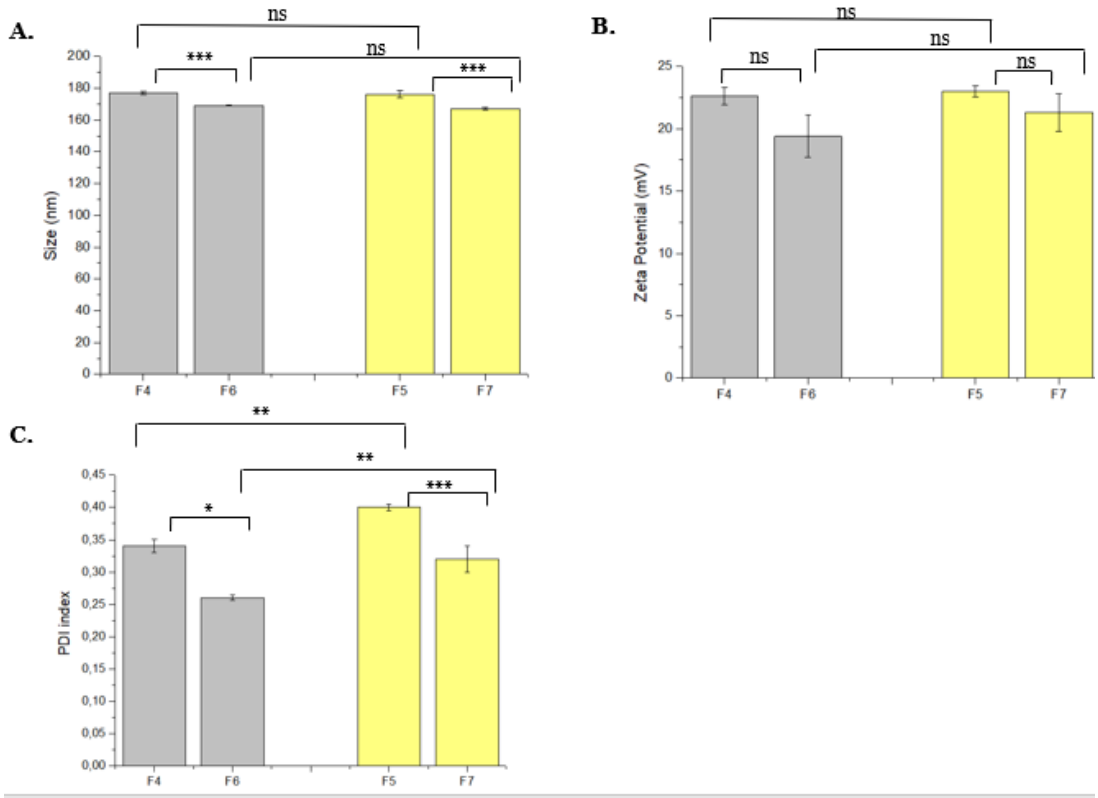

Figure 18. (A) Nanoparticles mean size (nm), **(B)** Average zeta potential, **(C)** Polydispersity index, changing CS volumes and TPP concentrations. The values were calculated with the data obtained from three independent measurements (mean ± S.D., n = 3) * $p < 0.05$; ** $p < 0.01$; *** $p < 0.001$; **** $p < 0.0001$, ns - no statistical difference.

From the results obtained in these experiments, concerning nanoparticles´ size, we concluded that the volume of CS does not affect this parameter, however, when decreasing the concentration of TPP smaller particles are obtained (Figure 18 A). This behavior was also observed by Bangun and co-workers, they concluded that increasing the TPP concentration led to precipitation or sedimentation in the solution, which suggested larger particle size. In their work, they showed the appearance of precipitation by analyzing the substance with the Fourier-transform infrared spectroscopy (FTIR) technique (Bangun, Tandiono, and Arianto 2018). Huang and Lapitsky showed in their study that aggregation kinetics are also slower at lower TPP concentrations, and lower pH values (Y. Huang and Lapitsky 2017).

The charge of the particles does not significantly change by increasing or decreasing the CS volume and TPP concentration, no statistical difference is observed in the results present in figure 18 **(B)**. Analyzing the obtained results, we can conclude that by decreasing the CS volume from 4 to 3 mL a decrease in PDI value is observed, as showed in figure 18 **(C)**. When the concentration of TPP decreases the same effect is noticed, which means more monodisperse nanoparticles are obtained.

4.5.3 Influence of changing CS concentration and volume with pDNA

Nanoparticles with and without pDNA were tested in lower CS concentration of 0.02% and 0.05% TPP with lower volume (250 µL) to confirm good conditions reached before. The formulations and results are described in table 12.

Table 12. Formulations changing CS concentration and volume after adding pDNA.

Formulation codes	CS Concentration (%)	CS Volume (mL)	Z - Average Size (nm)	PDI	Zeta Potential (mV)	Encapsulation efficiency (%)
F8	0.02	3	141 ± 3.96	0.24 ± 0.030	20.3 ± 0.92	Without pDNA
F9	0.02	2	121 ± 0.58	0.23 ± 0.011	20.5 ± 1.04	Without pDNA
F10	0.02	3	167 ± 1.35	0.23 ± 0.008	20.2 ± 0.76	78 ± 11.7
F11	0.02	2	179 ± 0.60	0.17 ± 0.004	20.0 ± 0.65	55 ± 9.3

[1] TPP concentration 0.05%, TPP volume 250 µL, pDNA concentration 20 µg/mL

Very good values were achieved with and without plasmid when analyzing the size, PDI, charge and encapsulation efficiency of the nanocarriers. In comparison to previous results, these conditions are the best ones achieved. The chosen parameters are 3 mL of 0.02% CS, 0.05% TPP volume of 250 µL with final pDNA concentration of 20 µg/mL. Using these conditions and parameters, all formulations are monodisperse with a PDI values below 0.25. An increase of 13% in encapsulation efficiency can be seen when increasing the CS volume from 2 mL to 3 mL.

The nanoparticles' size was smaller than 145 nm without pDNA and less than 180 nm after the pDNA addition. These results can be explained by the volume of TPP solution used (250 µL). As Rampino and colleagues also verified in their study, NPs aggregation occurred while using a high volume of TPP with a low volume of CS. They confirmed that increasing the amount of TPP into the CS solution led to flocculation or particle packing (Rampino et al. 2013). The same behavior was noticed by Masarudin and colleagues, in their study they showed that above 200 µL of TPP addition, the particle size and PDI increased significantly. They tested three different formulations, after 250 µL TPP addition, PDI values increased to 0.63 in CNP-F1, 0.79 in CNP-F2, and 0.64 in CNP-F3,

while an increase of 183, 231 and 205 nm in particle size for formulation 1, 2, and 3, respectively (Masarudin et al. 2015).

The decrease on NPs size can also be explained by the reduction on CS concentration from 0.035% to 0.02%. Same results were observed by Zaki and co-authors they evaluated the effects of different CS concentrations on particle size of CS nanoparticles (CSNPs) prepared from MMW and HMW CS. For MMW, particle size was increased with increasing CS concentration from 0.2% to 0.6% w/v. Particle size of HMW CSNPs was also significantly increased from 987 nm to 1651 nm when CS concentration was increased from 0.2% to 0.3% (Omar Zaki, Ibrahim, and Katas 2015). The same behavior was noticed by Tzeyung and co-authors they analyzed the effect of an increase in the CS concentration (0.05 to 0.15% w/v) on particle size, an increase in particle size was observed as the CS concentration increased. They suggested that this is because a high concentration of CS results in more CS chains per volume, thus forming larger particles when added with the cross-linking agent, TPP. It will also cause the cross-linking density between CS and TPP to decrease, resulting in particle aggregation and the formation of larger particles (Tzeyung et al. 2019).

Regarding the zeta potential, no difference is observed after the pDNA addition in both formulations. The nanoparticles were positively charged in all formulations with values around 20mV. Similar results concerning zeta potential values were found by Carrillo and co-authors, only a slight decrease was observed between the particles with and without the plasmid, although all formulations showed positive zeta potential values (Carrillo et al. 2014).

The charge of particles does not significantly change by increasing or decreasing the CS concentration from 0.035% to 0.02%. The same pattern was observed by Zaki and co-workers where they analyzed the effects of different CS concentrations on zeta potential of CS CSNPs prepared from MMW and HMW. For MMW zeta potential of these CSNPs was not significantly affected by CS concentration. Similar to MMW, CS concentration did not affect zeta potential of HMW CSNPs (Omar Zaki, Ibrahim, and Katas 2015).

4.5.4 Reproducibility and stability confirmation

Regarding the good results obtained in the last section, a triplicate of NPs formulated with 3 mL of 0.02% CS sample was performed with and without pDNA to confirm the reproducibility of this technique. TPP concentration of 0.05%, a volume of 250 μL and

pDNA concentration of 20 μg/mL were used for all formulations. The respective results are presented in Table 13.

Table 13. Triplicate formulation sample with the best results achieved to check the reproducibility and the stability of the systems performed.

	CS Concentration (%)	CS Volume (mL)	Z - Average Size (nm)	PDI	Zeta Potential (mV)	Encapsulation efficiency (%)
Particles freshly prepared	0.02 (1)	3	140 ± 1.75	0.23 ± 0.015	20.2 ± 1.32	Without pDNA
	0.02 (2)	3	146 ± 1.98	0.24 ± 0.019	20.3 ± 0.43	Without pDNA
	0.02 (3)	3	158 ± 3.02	0.22 ± 0.009	20.4 ± 0.40	Without pDNA
	0.02 (4)	3	172 ± 1.74	0.20 ± 0.008	21.7 ± 1.00	64 ± 7.8
	0.02 (5)	3	178 ± 1.19	0.17 ± 0.007	19.9 ± 0.38	67 ± 5.2
	0.02 (6)	3	175 ± 2.30	0.19 ± 0.016	19.6 ± 0.47	69± 4.1
After 72 h	0.02 (1)	3	157 ± 4.59	0.25 ± 0.017	23.4 ± 0.38	Without pDNA
	0.02 (2)	3	153 ± 1.24	0.26 ± 0.021	18.9 ± 3.20	Without pDNA
	0.02 (3)	3	168 ± 3.79	0.28 ± 0.011	21.2 ± 1.12	Without pDNA
	0.02 (4)	3	176 ± 0.94	0.24 ± 0.006	19.5 ± 0.78	62 ± 7.8
	0.02 (5)	3	185 ± 0.87	0.22 ± 0.012	20.3 ± 0.80	65 ± 5.2
	0.02 (6)	3	182 ± 3.14	0.20 ± 0.006	18.1 ± 1.08	68± 4.1
After 1 month	0.02 (1)	3	164 ± 6.32	0.24 ± 0.013	21.9 ± 0.24	Without pDNA
	0.02 (2)	3	155 ± 1.24	0.25 ± 0.009	19.7 ± 0.63	Without pDNA
	0.02 (3)	3	179 ± 3.79	0.26 ± 0.022	21.0 ± 1.07	Without pDNA
	0.02 (4)	3	177 ± 0.94	0.27 ± 0.008	22.3 ± 0.45	50 ± 7.8
	0.02 (5)	3	197 ± 0.87	0.21 ± 0.021	18.7 ± 0.59	52 ± 5.2
	0.02 (6)	3	188 ± 3.14	0.22 ± 0.003	20.1 ± 0.22	58 ± 4.1

All six formulations were prepared with fresh solutions of CS, TPP, and pDNA. The achieved system showed to be reproducible, since particles with and without plasmid DNA have very similar results in size, PDI, Zeta Potential, and encapsulation efficiency. An average increase of 30 nm in nanoparticles' size is noticed after adding the pDNA. Particles are still below 180 nm even after the addition of pDNA, good PDI, around 0.20, showing monodisperse particle population, and encapsulation efficiency above 65% considering the average of the three identical systems. Da Silva et al., presented very similar results using a low quantity of TPP inside the CS solution, in pH of 5.8, in which they had particles´ size in the range of 200 to 300 nm, with zeta potential values around 20 and 30 mV (da Silva et al. 2015).

According to Sreekumar and co-authors the reproducibility of the systems is still a problem that compromises the promising market applications of CS nanoparticles formed by the ionotropic gelation method. The initial CS concentration and the solvent atmosphere of the CS solution were the two main factors to create a reproducible system.

Their study showed that by understanding these two parameters reproducibility can be achieved. They were also capable of controlling the particles´ size by comprehending these two factors (Sreekumar et al. 2018).

Elgadir and his colleagues also found in other studies the feasibility of reproducible and stable nanoparticles´ systems that can encapsulate and deliver drugs. They mentioned that nanomedicine is a novelty regarding cancer treatment, diagnosis, and detection, and affirmed that polymer nanoparticles are promising drug carriers, their study showed *in-vitro* and *in-vivo* works that based and sustained their affirmation (Elgadir et al. 2015).

No difference is noticed in zeta potential values in particles with and without pDNA of Table 13. The charge of all formulations is around 20 mV showing very stable particles. The zeta potential evaluation can show the stability of the systems. The electrostatic force explains how this technique can suggest stability. If the zeta potential value of the particles is considerably high, this indicates that they will not attract each other creating a repulsion between them. In this way, aggregation or formation of clusters will be avoided. Nevertheless, if the zeta potential value of particles is not high enough to avoid the attraction between them, precipitates will be formed leading to unstable systems not only at the moment of the complexation but also, after some days or weeks (Santos-Carballal, Fernández Fernández, and Goycoolea 2018).

The stability of the nanocarriers was checked measuring the systems after 72 h and one month. Even after one month of storage in the refrigerator, the solution was clear and no aggregation and precipitation were noticed. The results regarding size, PDI and zeta potential showed in table 13 confirm that there is no significant variations throughout the time of the NPs storage. Moreover, the encapsulation efficiency of the polyplexes reduced around 14% in average, after one month. However, considering the charge of them, no significant difference is observed.

After the analysis of all parameters, these conditions were chosen as the best to proceed for stability and *in vitro* transfection studies with this pDNA delivery system.

4.5.5 Morphology of the polyplexes

The surface and morphology of CS-TPP-pDNA polyplexes were analyzed by scanning electron microscopy (SEM). The shape of nanoparticles can directly influence their

internalization into the cells. Figure 19 shows images of the nanocarriers developed with the best conditions mentioned above.

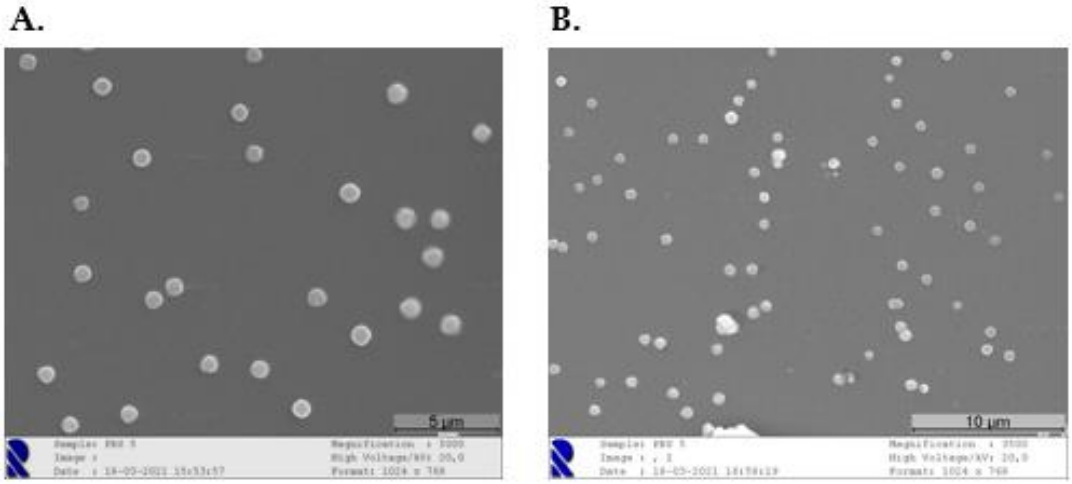

Figure 19. Scanning electron micrographs of CS-TPP-pDNA E7 nanoparticles formulated with the best conditions reached. **(A)** Magnification of 5000, **(B)** Magnification of 3500.

From figure 19 we can see that all nanocarriers present spherical or oval shape particles in nano sizes, lower than 200 nm. The morphology presented by the best-chosen formulation is suitable for cellular uptake and internalization. Several studies described in the literature that spherical and oval nanoparticles shape have benefits in comparison to rod shapes, especially showing higher cellular uptake/transfection efficiency. For instance, Zhang and colleagues showed that nanoparticles of poly(acrylic acid)-*b*-polystyrene with spherical morphology had presented greater cellular internalization by the Chinese hamster ovary cells (CHO) in comparison to nanoparticles with rod shape (Zhang et al. 2008). Different kinds of nanoparticles, especially gold NPs, were evaluated by Chithrani and co-workers and also showed the same phenomenon confirming that gold spheres had more uptake results in HeLa cells, when compared with rod-shaped particles (Chithrani, Ghazani, and Chan 2006).

4.5.6 Stability tests

Electrophoresis consists of a frequently used method to isolate different macromolecules regarding their size and charge, this technique is regularly used on proteins and nucleic acids. As it was mentioned before, nucleic acids are very negatively charged because of their phosphate groups, the application of an electric field between positive and negative polarity will make these molecules move. The way and how fast these molecules move through the gel is dependent by the molecular weight. This methodology was used in this work to evaluate the samples resultant from the stability studies of nanoparticles with plasmid DNA encapsulated. This assay can also be used to identify the adsorption or encapsulation efficiency of nucleic acids to CS polymer, while the production process of

systems, or to analyze the protection offered by nanoparticles to the pDNA inside them (Santos-Carballal, Fernández Fernández, and Goycoolea 2018).

The stability test was performed with the triplicates of NPs with pDNA showed in the results above (Table 13) using the best parameters defined. The assay was performed at three different incubation times (0, 2 and 6 h) to evaluate the behavior of naked pDNA and nanoparticles in contact with DMEM-F12 medium supplemented with 10% of serum (FBS) and trypsin. The electrophoresis technique was used to analyze the supernatant of each incubation and detect the presence of plasmid, which indicates the NPs decomplexation. In addition, the incubation of free pDNA in previously described conditions can result in pDNA degradation, which is visible by the presence of some small and linear pieces through the electrophoretic migration, indicating the instability of the NPs (Santos et al. 2014). Figure 20 shows the obtained results.

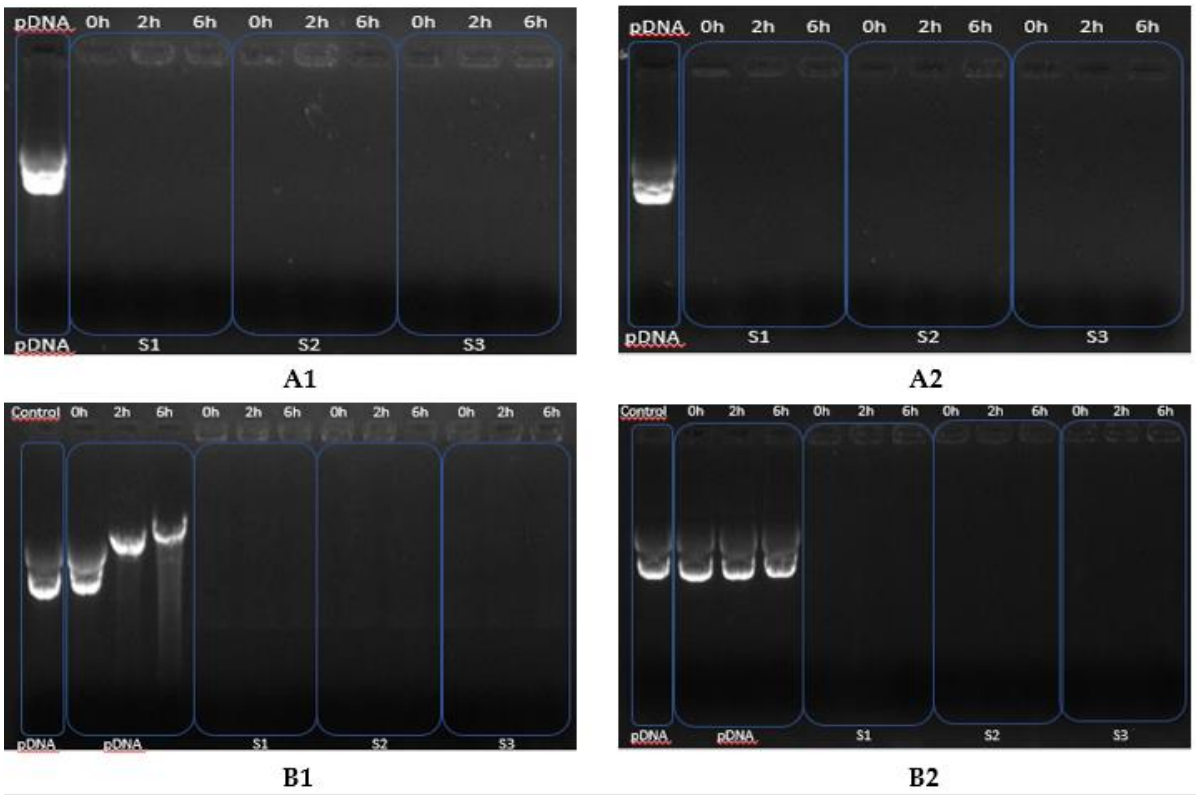

Figure 20. Electrophoretic analysis of the supernatants of the nanoparticles without medium **(A1)** and without trypsin **(A2)**. Lane 1: pDNA control, lane 2 - 10: non-encapsulated pDNA samples 1, 2 and 3, incubation of 0, 2 and 6 h. Electrophoretic analysis of the system's protection of pDNA after its incubation with DMEM-F12 medium supplemented with 10 % of serum FBS **(B1)** and after its incubation with trypsin in **(B2)**. Lane 1: pDNA control; lane 2 - 4: pDNA with medium, at 0, 2, and 6 h. Lane 5 -13: CS-TPP-pDNA sample 1, 2, and 3 with medium at 0, 2, and 6 h; Figure **(B2)**: same order, with trypsin.

The supernatants of three samples were evaluated to check the encapsulation efficiency of the systems. From the result, no free DNA is observed in the agarose gel for all samples evidencing that very high amount of plasmid added should be entrapped into the CS-

TPP-pDNA polyplexes and some small amount of remaining complexes can be seen in the gel wells depicted in picture 20 **(A1)** and **(A2)**. This can be explained due to the fact that not 100% of plasmid DNA was encapsulated inside the nanoparticles some of the content may stay in the supernatant solution or even attached to the outside surface of the nanocarriers by adsorption. Similar results were also reported by Carrillo and co-workers, no free DNA was observed in the gel even for different CS concentrations and for different plasmid volumes (Carrillo et al. 2014).

After 6 h incubation with medium continuously degradation of naked pDNA is observed along the time in lanes 3, 4, and 5 in picture 20 **(B1)**. However, analyzing the other lanes in which the pDNA is encapsulated inside the nanocarriers, no free DNA is observed in the electrophoretic mobility. These results suggests that the CS-pDNA-TPP nanoparticles did not destabilize during these incubations and effectively protect the plasmid, and consequently the E7 trangene, from degradation at least 6 during hours. Picture 20 **(B2)** evidences that no disruption happens in nanoparticles during 6 h of incubation with trypsin, due to the nonappearance of pDNA bands in electrophoresis image, and no degradation is observed of the naked pDNA.

Another study to evaluate the stability was performed with Dulbecco´s Modified Eagle´s Medium with High Glucose (DMEM-HG) supplemented with 10% not inactivated fetal bovine serum and trypsin. The analyzes were done after 6 h of incubation with both excipients and the NPs were degraded to confirm encapsulation and release of encapsulated pDNA.

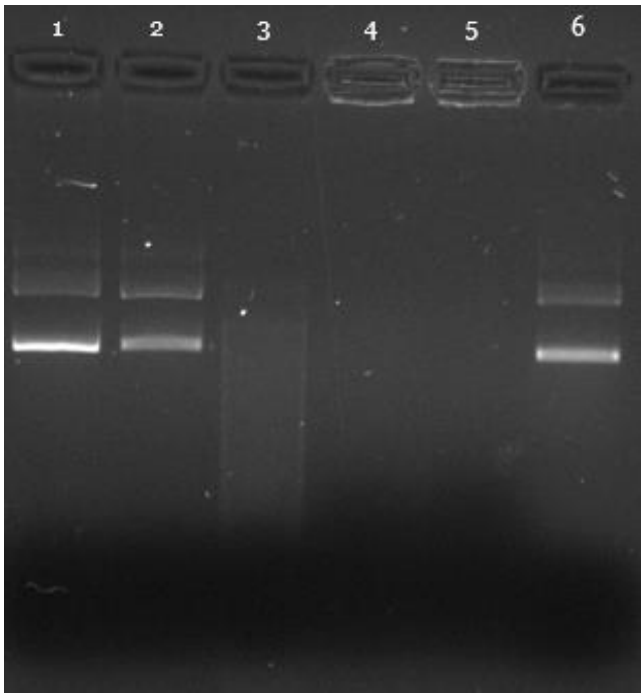

Figure 21. Electrophoretic analysis of the naked pDNA after 6 h incubation with trypsin and medium, nanoparticles with encapsulated pDNA after 6 h incubation with trypsin and medium, and decomplexated NPs after 6 h incubation with medium. Lane 1: naked pDNA control 0 h, lane 2: pDNA incubated 6 h with trypsin, lane 3: pDNA incubated 6 h with medium, lane 4: NPs incubated 6h with trypsin, lane 5: NPs incubated 6 h with medium, lane 6: decomplexated NPs.

After 6 h incubation with medium complete degradation of naked pDNA in lane 3 is noticed, however, after 6 h incubation with trypsin naked pDNA remains without degradation. Evaluating the other lanes in which the pDNA is encapsulated inside the nanocarriers, no free DNA is observed in the electrophoretic mobility. These results suggest that even with medium or trypsin the CS-pDNA-TPP nanoparticles did not destabilize during these incubations and effectively protect the plasmid, and consequently the E7 transgene, from degradation at least 6 hours. After the analysis of the complete degradation of naked pDNA in contact with DMEM-HG medium after 6 h incubation an experiment was performed with pDNA encapsulated inside the polyplexes incubated in medium for 6 h. NPs were decomplexated using the dEE method described before. Briefly, 1 mL of 2% acetic acid and an additional 100 μL of 2 M HCl were added to the pellet for nanoparticle decomplexation and release of encapsulated DNA to confirm the protection of pDNA inside the nanocarriers. After the vector's decomplexation, the result suggests that the pDNA remains unadulterated after 6 h showing that the system is effective to protect pDNA from medium degradation, the result also confirms the pDNA encapsulation and release after particle deterioration.

4.5.7 Cell viability evaluation

In vitro tests of cell viability in the presence of NPs are very important to prognosticate what can happen in the human response. These tests evaluate the capability of relevant cells to maintain metabolically activity in the presence of particular materials or carriers and also provide consistent information on how these systems will behave in a biological habitat (Rodrigues et al. 2012).

Cellular cytotoxicity is one of the most important issues to be analyzed when choosing the best delivery system, if the system has high toxicity, it cannot be used for gene transfection purposes or therapeutic assays. The resazurin cell viability or also called alamar blue is a fluorescent experiment to identify the metabolism activity of the cells. This compound is known for its low cytotoxic and its ability to dye the cells. The conversion of resazurin with blue color into resorufin with pink fluorescent color can only happen in viable cells (Gong et al. 2020). In this context, to determine the toxicity levels of formulations, the resazurin experiment was performed on fibroblasts and raw cells for 24 and 48 hours.

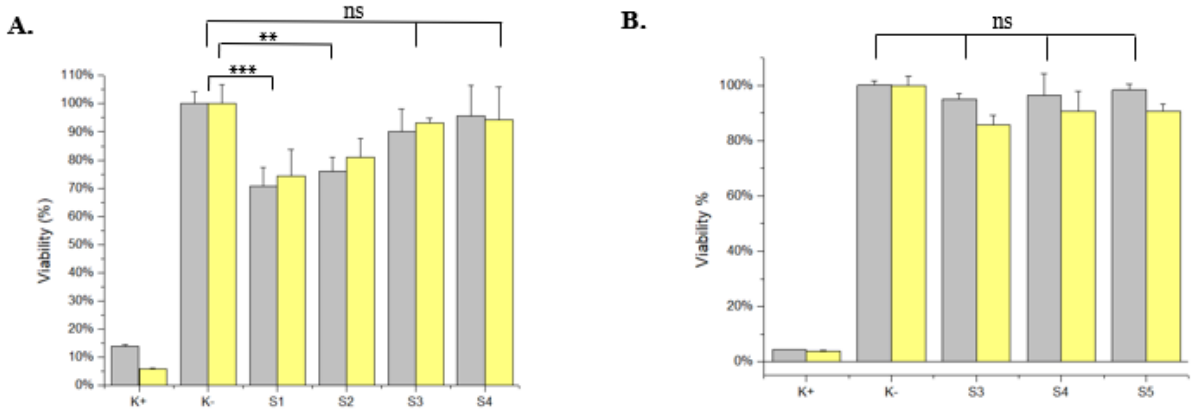

Figure 22. Cell viability after 24 h (gray) and 48 h (yellow) of transfection with CS-TPP-pDNA polyplexes, for Fibroblasts cells **(A)** and for Raw cells **(B)**. S1 – NPs centrifuged at 2000 RCF, 10 minutes, DNA concentration of 20 µg/mL; S2 - NPs centrifuged at 4000 RCF, 10 minutes, DNA concentration of 20 µg/Ml; S3 - NPs centrifuged at 6000 RCF, 10 minutes, DNA concentration of 20 µg/mL. S4 - NPs centrifuged at 10000 RCF, 10 minutes, DNA concentration of 20 µg/mL; S5 - NPs centrifuged at 10000 RCF, 10 minutes, DNA concentration of 60 µg/mL. Non-transfected cells were used as negative control (K-) and ethanol-treated cells were used as positive controls (K+) for cytotoxicity. Statistical analysis was made using "one-way ANOVA" with data obtained from three independent measurements (mean ± SD, n = 3). The asterisks symbol represents statistical significance (** $p \leq 0.01$; *** $p \leq 0.001$), ns – no statistical difference.

For the fibroblast cells, four different centrifugation speeds were done before the resuspension of the pellets with medium for the cell transfection. The results depicted in figure 22 **(A)** show a very significant difference between the four samples. Considering 80% or higher values as acceptable results, statistical difference is noticed between samples 1 and 2 and the negative control. This result suggests these NPs samples present

potential toxicity for healthy cells and could be a considerable problem for future applications.

The cytotoxicity presented can be explained due to the fact of lower centrifugation speed used (2000 RCF and 4000 RCF). Considering that CS and TPP solutions are both prepared in acidic conditions, using these speeds the systems must not get rid off the impurities. Lazaridou and co-authors, in their study also prepared their systems by the ionotropic gelation method and used higher centrifugation speed (13000 RPM) to completely remove the non-entrapped drug and dissolved CS from the nanoparticles systems (Lazaridou et al. 2020).

The same conditions were performed to samples S3 and S4 for Fibroblasts, being the only difference of the increased centrifuge speed (to 6000 and 10000 RCF) and no statistical difference was found between control and samples in the 2 days evaluated. These results suggest that these polyplexes do not induce cytotoxicity. For the viability assays of raw cells, we chose the 2 best centrifuge speeds (6000 and 10000 RCF), and one test with the triple DNA concentration (60 μg/mL). Again, the results confirm no statistical difference between control and all systems done, supporting that no cytotoxicity is induced.

Valente and co-authors compared the cytotoxicity between two systems (PEI and CS nanoparticles) in their study made in HeLa cancer cells and human dermal fibroblasts (hFib) proved that CH-based polyplexes loaded with different pDNA did not lead cytotoxicity and also recommended the CS-based systems as safer for pDNA delivery than PEI-based (Valente et al. 2021). Da Silva and colleagues, also prepared CS nanoparticles using the ionotropic gelation technique to encapsulate rosmarinic acid. The particles showed low cytotoxicity against the retinal pigments and the corneal cells. They concluded that CS nanoparticles are a promising method for the release of drugs in ocular applications (da Silva et al. 2015).

4.5.8 E7 gene expression

After transfection of fibroblasts and raw cells by the developed gene delivery systems, E7 mRNA expression in transfected cells was evaluated. Firstly, total RNA was extracted, then the RNA was reverse transcribed into cDNA, and RT-PCR experiment was performed to amplify the E7 gene using specific primers. The products of the obtained PCR were visualized by electrophoresis in 1% agarose gel. For both experiments, three different pDNA concentrations were used 20, 40 and 60 μg/mL. Untreated cells were

used as negative control and also a mixture control without cDNA was used to detect any kind of contamination. The result is shown in figure 23 **(A)** and **(B)** below.

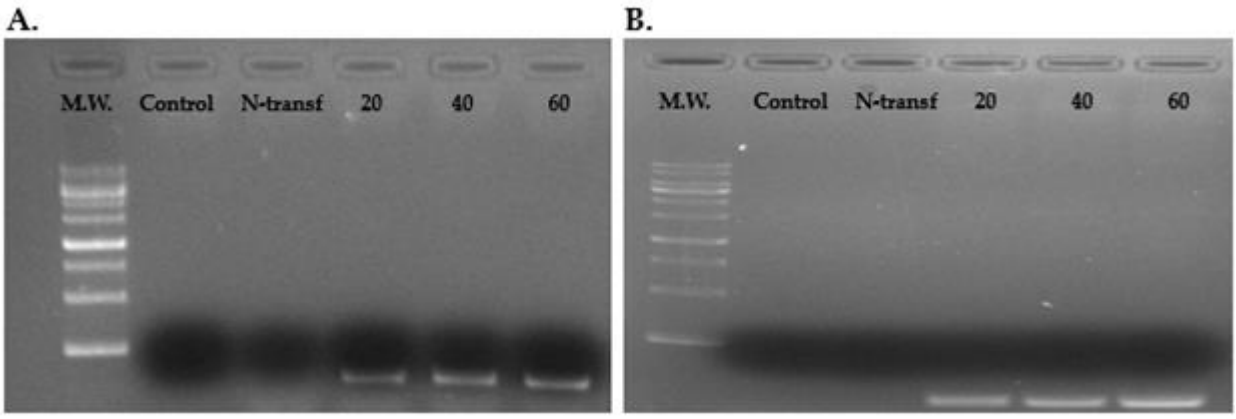

Figure 23. Analysis of RT-PCR products by agarose gel electrophoresis. Evaluation of E7 transcripts in Fibroblasts cells **(A)** and Raw cells **(B)**. Lane 1: DNA molecular weight marker; lane 2: control without cDNA sample; lane 3: non-transfected cells; lane 4: cells transfected by CS-TPP-pDNA [20 μg/mL]; lane 5: cells transfected by CS-TPP-pDNA [40 μg/mL]; lane 6: cells transfected by CS-TPP-pDNA [60 μg/mL].

Considerable and intense levels of mRNA of the protein E7 from transfected cells were observed for all CS-TPP-pDNA systems. No band is detected in both negative controls. In the second lane the result of no band expressed implies that no contamination happened during the assays and in the third lane suggests that the non-transfected cells do not promote the gene expression. For both results, while increasing the pDNA concentration more intense band is noticed. The RT-PCR technique demonstrated that the produced nanoparticles have the desired and intended effect. The formulated systems show very good protection to the pDNA through the transfection process and arrival to the nucleus because of the interest gene transcription.

RT-qPCR experiment was performed to quantify E7 gene expression levels, this assay is more accurate and specific allowing the comparison and evaluation of two different samples with two different centrifugation speeds (6000 and 10000 RCF). The results for gene expression of both polyplexes, after transfection, are depicted in Figure 24 below.

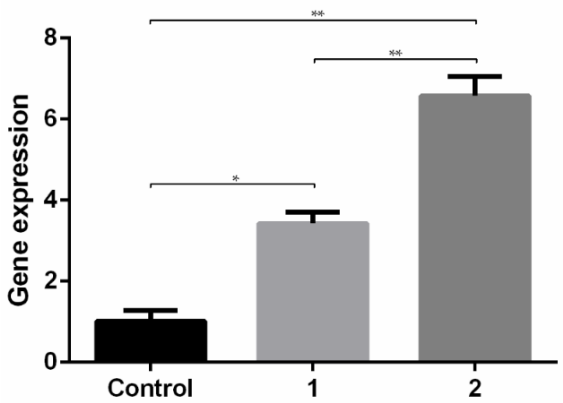

Figure 24. RT-qPCR of E7 expression levels in RAW cells. Control – non-transfected cells; 1- CS-TPP-pDNA, centrifugation speed 6000 RCF, pDNA concentration of 60 μg/mL; 2- CS-TPP-pDNA, centrifugation speed 10000 RCF, pDNA concentration of 60 μg/mL. Data obtained from three independent measurements (mean ± S.D., n = 3). * $p < 0.05$; ** $p < 0.01$

From the results of cell viability, two systems were non-toxic to the cells, centrifuge at 6000 RCF and 10000 RCF and increasing the pDNA concentration from 20 to 60 μg/mL no difference was detected, showing that an increase in the pDNA concentration does not lead to an increase in cell viability. From the PCR tests more intense band was noticed using the pDNA concentration of 60 μg/mL in comparison to other two less concentrated samples. From figure 24 above, there is an increase in the expression of E7 transcripts in relation to non-transfected cells (control) for both systems. CS-TPP-pDNA polyplexes centrifuged at 10000 RCF show higher levels of E7 transcripts in cells when compared to the polyplexes centrifuged at 6000 RCF, proving that the centrifugation speed may play a crucial role in influencing the viability and consequently the degree of cellular internalization of the polyplexes. The results suggest that these are the best conditions for an efficient cellular internalization/uptake. This fact and all the others analyzed, make clear the success of gene expression and consequently, protein expression and, therefore, therapeutic effect.

5 Conclusions and future perspectives

The development of new therapies for the treatment of cervical cancer has emerged as an object of investigation in several studies. Currently, cervical cancer is the 4th largest cause of cancer in women worldwide. Nowadays is considered one of the most common public health issue, principally in middle-aged women group, especially in less developed countries. Some specific actions have been made to reduce cervical cancer rates, such as sexual education campaigns by the government, improvement of HPV vaccination, easier access to cancer screening tests, and immunotherapy treatment. Since cancer is increasing exponentially all over the world and the prophylactic vaccines cannot treat or revert cancers induced by pre-existing and persistent HPV infections, it is necessary to develop new strategies that can overcome the limitations of these vaccines. In this way, DNA vaccination is a promising approach because allows the prevention and treatment of pre-existed diseases, additionally, they are safer and more effective than the traditional vaccines being applicable against a great range of viral, bacterial, and parasitic diseases, including the cervical cancer induced by HPV.

In order to contribute to the progress of cancer therapies, specifically cervical cancer, the approach of this master research project is focused on the development of polyplexes systems to deliver plasmid DNA. In this work, the ionotropic gelation technique was used to formulate nanoparticles that are able to encapsulate and protect pDNA. The obtained results revealed that many parameters have to be taken into account when developing these gene delivery vehicles. Among the different conditions and parameters, the volume and concentration of CS and tripolyphosphate (TPP) showed to have the most important role in the design of the nanoparticles' size, encapsulation efficiency, and surface charge. Together, these two parameters must be combined and associated to achieve a balance between encapsulation, size, non-aggregation, surface charge, and transfection efficiency. The findings presented in this work reveal that the nanocarriers have a high pDNA encapsulation efficiency rate, nanometric sizes, spherical/oval shape, and positive surface charge, suitable characteristics for pDNA vaccine delivery protocols for cervical cancer treatment.

The present work demonstrated that the delivery systems formulated with the ionotropic gelation approach using CS as a polymer and TPP as polyanionic crosslinker can be considered as good candidates to develop potential administration of genes in order to

achieve good and satisfactory results for effective DNA based therapies, contributing to the evolution and success of medical treatment against cervical cancer. However, it is still necessary to focus the investigation on these systems to complete the obtained results with the specific determination of the E7 protein using the western blot experiment. Another approach that can be explored in the future is the evaluation of mucopenetration/mucoadhesion property of the CS polyplexes which give the advantage of prolonging the residence time in the mucosal areas, offering advantages for mucosal drug delivery, especially in the place that the absorption happens making the vehicles promising for less invasive administration.

6 References

Agirre, Mireia, Jon Zarate, Edilberto Ojeda, Gustavo Puras, Jacques Desbrieres, and Jose Luis Pedraz. 2014. “Low Molecular Weight CS (LMWC)-Based Polyplexes for PDNA Delivery: From Bench to Bedside.” *Polymers* 6 (6): 1727–55. https://doi.org/10.3390/polym6061727.

Al-nemrawi, N K, S S M Alsharif, and R H Dave. 2018. “ Preparation of CS-tpp nanoparticles: the influence of CS polymeric properties and formulation variables.” *International Journal of Applied Pharmaceutics* 10 (5): 60–65. https://doi.org/10.22159/ijap.2018v10i5.26375.

Almeida, Ana M, João A Queiroz, Fani Sousa, and Ângela Sousa. 2019. “Cervical Cancer and HPV Infection: Ongoing Therapeutic Research to Counteract the Action of E6 and E7 Oncoproteins.” *Drug Discovery Today* 24 (10): 2044–57. https://doi.org/10.1016/j.drudis.2019.07.011.

Almeida, Ana M, Joana Tomás, Patrícia Pereira, João A Queiroz, Fani Sousa, and Ângela Sousa. 2018. “HPV-16 Targeted DNA Vaccine Expression: The Role of Purification.” *Biotechnology Progress* 34 (2): 546–51. https://doi.org/https://doi.org/10.1002/btpr.2603.

Anderson, Richard J, and Joerg Schneider. 2007. “Plasmid DNA and Viral Vector-Based Vaccines for the Treatment of Cancer.” *Vaccine* 25 Suppl 2 (September): (B2)4-34. https://doi.org/10.1016/j.vaccine.2007.05.030.

Arbyn, Marc, Elisabete Weiderpass, Laia Bruni, Silvia de Sanjosé, Mona Saraiya, Jacques Ferlay, and Freddie Bray. 2020. “Estimates of Incidence and Mortality of Cervical Cancer in 2018: A Worldwide Analysis.” *The Lancet. Global Health* 8 (2): e191–203. https://doi.org/10.1016/S2214-109X(19)30482-6.

Badawy, Mohamed E I, and Entsar I Rabea. 2011. “A Biopolymer CS and Its Derivatives as Promising Antimicrobial Agents against Plant Pathogens and Their Applications in Crop Protection.” Edited by Bruno Sarmento. *International Journal of Carbohydrate Chemistry* 2011: 460381. https://doi.org/10.1155/2011/460381.

Badazhkova, Veronika D, Sergei V Raik, Dmitry S Polyakov, Daria N Poshina, and Yury A Skorik. 2020. “Effect of Double Substitution in Cationic CS Derivatives on DNA Transfection Efficiency.” *Polymers* 12 (5). https://doi.org/10.3390/polym12051057.

Baden, Lindsey R, Hana M El Sahly, Brandon Essink, Karen Kotloff, Sharon Frey, Rick Novak, David Diemert, et al. 2021. “Efficacy and Safety of the MRNA-1273 SARS-

CoV-2 Vaccine." *The New England Journal of Medicine* 384 (5): 403–16. https://doi.org/10.1056/NEJMo(A2)035389.

Bangun, Hakim, Steve Tandiono, and Anayanti Arianto. 2018. "Preparation and Evaluation of CS-Tripolyphosphate Nanoparticles Suspension as an Antibacterial Agent." *Journal of Applied Pharmaceutical Science*, no. Volume: 8, Issue: 12: 147–56. http://japsonline.com/abstract.php?article_id=2794.

Bellich, Barbara, Ilenia D'Agostino, Sabrina Semeraro, Amelia Gamini, and Attilio Cesàro. 2016. "'The Good, the Bad and the Ugly' of CSs." *Marine Drugs* 14 (5). https://doi.org/10.3390/md14050099.

Cao, Ye, Yang Fei Tan, Yee Shan Wong, Melvin Wen Jie Liew, and Subbu Venkatraman. 2019. "Recent Advances in CS-Based Carriers for Gene Delivery." *Marine Drugs* 17 (6). https://doi.org/10.3390/md17060381.

Carrillo, Carolina, Josep Maria Suñé, Pilar Pérez-Lozano, Encarna García-Montoya, Rocío Sarrate, Anna Fàbregas, Montserrat Miñarro, and Josep Ramon Ticó. 2014. "CS Nanoparticles as Non-Viral Gene Delivery Systems: Determination of Loading Efficiency." *Biomedicine & Pharmacotherapy* 68 (6): 775–83. https://doi.org/https://doi.org/10.1016/j.biopha.2014.07.009.

Chabeda, Aleyo, Romana J R Yanez, Renate Lamprecht, Ann E Meyers, Edward P Rybicki, and Inga I Hitzeroth. 2018. "Therapeutic Vaccines for High-Risk HPV-Associated Diseases." *Papillomavirus Research (Amsterdam, Netherlands)* 5 (June): 46–58. https://doi.org/10.1016/j.pvr.2017.12.006.

Chandra Hembram, Krushna, Shashi Prabha, Ramesh Chandra, Bahar Ahmed, and Surendra Nimesh. 2016. "Advances in Preparation and Characterization of CS Nanoparticles for Therapeutics." *Artificial Cells, Nanomedicine, and Biotechnology* 44 (1): 305–14. https://doi.org/10.3109/21691401.2014.948548.

Chauhan, Abhay Singh. 2018. "Dendrimers for Drug Delivery." *Molecules (Basel, Switzerland)* 23 (4). https://doi.org/10.3390/molecules23040938.

Chen, Chih-Kuang, Ping-Kuan Huang, Wing-Cheung Law, Chia-Hui Chu, Nai-Tzu Chen, and Leu-Wei Lo. 2020. "Biodegradable Polymers for Gene-Delivery Applications." *International Journal of Nanomedicine* 15: 2131–50. https://doi.org/10.2147/IJN.S222419.

Chen, Kuo-Yu, and Si-Ying Zeng. 2018. "Fabrication of Quaternized CS Nanoparticles Using Tripolyphosphate/Genipin Dual Cross-Linkers as a Protein Delivery System." *Polymers* 10 (11). https://doi.org/10.3390/polym10111226.

Cheng, Liqin, Yan Wang, and Juan Du. 2020. "Human Papillomavirus Vaccines: An Updated Review." *Vaccines* 8 (3). https://doi.org/10.3390/vaccines8030391.

Chithrani, B Devika, Arezou A Ghazani, and Warren C W Chan. 2006. "Determining the Size and Shape Dependence of Gold Nanoparticle Uptake into Mammalian Cells." *Nano Letters* 6 (4): 662–68. https://doi.org/10.1021/nl052396o.

Christoforidis, John B, Susie Chang, Angela Jiang, Jillian Wang, and Colleen M Cebulla. 2012. "Intravitreal Devices for the Treatment of Vitreous Inflammation." Edited by Mario R Romano. *Mediators of Inflammation* 2012: 126463. https://doi.org/10.1155/2012/126463.

Csaba, Noemi, Magnus Köping-Höggård, and Maria Jose Alonso. 2009. "Ionically Crosslinked CS/Tripolyphosphate Nanoparticles for Oligonucleotide and Plasmid DNA Delivery." *International Journal of Pharmaceutics* 382 (1–2): 205–14. https://doi.org/10.1016/j.ijpharm.2009.07.028.

Danaei, M, M Dehghankhold, S Ataei, F Hasanzadeh Davarani, R Javanmard, A Dokhani, S Khorasani, and M R Mozafari. 2018. "Impact of Particle Size and Polydispersity Index on the Clinical Applications of Lipidic Nanocarrier Systems." *Pharmaceutics* 10 (2). https://doi.org/10.3390/pharmaceutics10020057.

Das, Surajit, and Anumita Chaudhury. 2011. "Recent Advances in Lipid Nanoparticle Formulations with Solid Matrix for Oral Drug Delivery." *AAPS PharmSciTech* 12 (1): 62–76. https://doi.org/10.1208/s12249-010-9563-0.

Doorbar, John, Nagayasu Egawa, Heather Griffin, Christian Kranjec, and Isao Murakami. 2015. "Human Papillomavirus Molecular Biology and Disease Association." *Reviews in Medical Virology* 25 Suppl 1 (Suppl Suppl 1): 2–23. https://doi.org/10.1002/rmv.1822.

Elgadir, M.Abd, Md.Salim Uddin, Sahena Ferdosh, Aishah Adam, Ahmed Jalal Khan Chowdhury, and Md.Zaidul Islam Sarker. 2015. "Impact of CS Composites and CS Nanoparticle Composites on Various Drug Delivery Systems: A Review." *Journal of Food and Drug Analysis* 23 (4): 619–29. https://doi.org/https://doi.org/10.1016/j.jfda.2014.10.008.

Ensign, Laura M, Richard Cone, and Justin Hanes. 2012. "Oral Drug Delivery with Polymeric Nanoparticles: The Gastrointestinal Mucus Barriers." *Advanced Drug Delivery Reviews* 64 (6): 557–70. https://doi.org/10.1016/j.addr.2011.12.009.

Ensign, Laura M, Craig Schneider, Jung Soo Suk, Richard Cone, and Justin Hanes. 2012. "Mucus Penetrating Nanoparticles: Biophysical Tool and Method of Drug and Gene Delivery." *Advanced Materials* 24 (28): 3887–94. https://doi.org/https://doi.org/10.1002/adma.201201800.

Ezzati Nazhad Dolatabadi, Jafar, Hadi Valizadeh, and Hamed Hamishehkar. 2015. "Solid Lipid Nanoparticles as Efficient Drug and Gene Delivery Systems: Recent

Breakthroughs." *Advanced Pharmaceutical Bulletin* 5 (2): 151–59. https://doi.org/10.15171/apb.2015.022.

Fan, Yuchen, and Qiang Zhang. 2013. "Development of Liposomal Formulations: From Concept to Clinical Investigations." *Asian Journal of Pharmaceutical Sciences* 8 (2): 81–87. https://doi.org/https://doi.org/10.1016/j.ajps.2013.07.010.

Farris, Eric, Deborah M Brown, Amanda E Ramer-Tait, and Angela K Pannier. 2016. "Micro- and Nanoparticulates for DNA Vaccine Delivery." *Experimental Biology and Medicine (Maywood, N.J.)* 241 (9): 919–29. https://doi.org/10.1177/1535370216643771.

Geszke-Moritz, Małgorzata, and Michał Moritz. 2016. "Solid Lipid Nanoparticles as Attractive Drug Vehicles: Composition, Properties and Therapeutic Strategies." *Materials Science & Engineering. C, Materials for Biological Applications* 68 (November): 982–94. https://doi.org/10.1016/j.msec.2016.05.119.

Gheit, Tarik. 2019. "Mucosal and Cutaneous Human Papillomavirus Infections and Cancer Biology." *Frontiers in Oncology* 9: 355. https://doi.org/10.3389/fonc.2019.00355.

Gómez, Leonardo A, and Angel A Oñate. 2019. "Plasmid-Based DNA Vaccines." In *Plasmid*, edited by Munazza Gull. Rijeka: IntechOpen. https://doi.org/10.5772/intechopen.76754.

Gong, Xianghui, Zhuqing Liang, Yongxing Yang, Haifeng Liu, Jing Ji, and Yubo Fan. 2020. "A Resazurin-Based, Nondestructive Assay for Monitoring Cell Proliferation during a Scaffold-Based 3D Culture Process." *Regenerative Biomaterials* 7 (3): 271–81. https://doi.org/10.1093/rb/rbaa002.

Graham, Sheila V. 2010. "Human Papillomavirus: Gene Expression, Regulation and Prospects for Novel Diagnostic Methods and Antiviral Therapies." *Future Microbiology* 5 (10): 1493–1506. https://doi.org/10.2217/fmb.10.107.

Gulce-Iz, Sultan, and Pelin Saglam-Metiner. 2019. "Current State of the Art in DNA Vaccine Delivery and Molecular Adjuvants: Bcl-XL Anti-Apoptotic Protein as a Molecular Adjuvant." In *Immune Response Activation and Immunomodulation*, edited by Rajeev K Tyagi and Prakash S Bisen. Rijeka: IntechOpen. https://doi.org/10.5772/intechopen.82203.

Ha, S-J, B-Y Jeon, J-I Youn, S-C Kim, S-N Cho, and Y-C Sung. 2005. "Protective Effect of DNA Vaccine during Chemotherapy on Reactivation and Reinfection of Mycobacterium Tuberculosis." *Gene Therapy* 12 (7): 634–38. https://doi.org/10.1038/sj.gt.3302465.

Huang, Kuo-Shien, Yea-Ru Sheu, and In-Chun Chao. 2009. "Preparation and

Properties of NanoCS." *Polymer-Plastics Technology and Engineering* 48 (12): 1239–43. https://doi.org/10.1080/03602550903159069.

Huang, Yan, and Yakov Lapitsky. 2017. "On the Kinetics of CS/Tripolyphosphate Micro- and Nanogel Aggregation and Their Effects on Particle Polydispersity." *Journal of Colloid and Interface Science* 486: 27–37. https://doi.org/https://doi.org/10.1016/j.jcis.2016.09.050.

Ibraheem, D, A Elaissari, and H Fessi. 2014. "Gene Therapy and DNA Delivery Systems." *International Journal of Pharmaceutics* 459 (1–2): 70–83. https://doi.org/10.1016/j.ijpharm.2013.11.041.

Jumaa, M, and B W Müller. 2000. "Lipid Emulsions as a Novel System to Reduce the Hemolytic Activity of Lytic Agents: Mechanism of the Protective Effect." *European Journal of Pharmaceutical Sciences : Official Journal of the European Federation for Pharmaceutical Sciences* 9 (3): 285–90. https://doi.org/10.1016/s0928-0987(99)00071-8.

Kim, Sae-Hae, Kyung-Yeol Lee, and Yong-Suk Jang. 2012. "Mucosal Immune System and M Cell-Targeting Strategies for Oral Mucosal Vaccination." *Immune Network* 12 (5): 165–75. https://doi.org/10.4110/in.2012.12.5.165.

Kutzler, Michele A, and David B Weiner. 2008. "DNA Vaccines: Ready for Prime Time?" *Nature Reviews Genetics* 9 (10): 776–88. https://doi.org/10.1038/nrg2432.

Lai, Samuel K, Ying-Ying Wang, and Justin Hanes. 2009. "Mucus-Penetrating Nanoparticles for Drug and Gene Delivery to Mucosal Tissues." *Advanced Drug Delivery Reviews* 61 (2): 158–71. https://doi.org/10.1016/j.addr.2008.11.002.

Lazaridou, Maria, Evi Christodoulou, Maria Nerantzaki, Margaritis Kostoglou, Dimitra A Lambropoulou, Angeliki Katsarou, Kostas Pantopoulos, and Dimitrios N Bikiaris. 2020. "Formulation and In-Vitro Characterization of CS-Nanoparticles Loaded with the Iron Chelator Deferoxamine Mesylate (DFO)." *Pharmaceutics* 12 (3). https://doi.org/10.3390/pharmaceutics12030238.

Lee, Jihui, Shreedevi Arun Kumar, Yong Yu Jhan, and Corey J Bishop. 2018. "Engineering DNA Vaccines against Infectious Diseases." *Acta Biomaterialia* 80 (October): 31–47. https://doi.org/10.1016/j.actbio.2018.08.033.

Li, Shyh-Dar, and Leaf Huang. 2008. "Pharmacokinetics and Biodistribution of Nanoparticles." *Molecular Pharmaceutics* 5 (4): 496–504. https://doi.org/10.1021/mp800049w.

Lim, Michael, Abu Zayed Md Badruddoza, Jannatul Firdous, Mohammad Azad, Adnan Mannan, Taslim Ahmed Al-Hilal, Chong-Su Cho, and Mohammad Ariful Islam.

2020. “Engineered Nanodelivery Systems to Improve DNA Vaccine Technologies.” *Pharmaceutics* 12 (1). https://doi.org/10.3390/pharmaceutics12010030.

Lin, Chih-Hung, Chun-Han Chen, Zih-Chan Lin, and Jia-You Fang. 2017. “Recent Advances in Oral Delivery of Drugs and Bioactive Natural Products Using Solid Lipid Nanoparticles as the Carriers.” *Journal of Food and Drug Analysis* 25 (2): 219–34. https://doi.org/10.1016/j.jfda.2017.02.001.

Liu, Min, Jian Zhang, Wei Shan, and Yuan Huang. 2015. “Developments of Mucus Penetrating Nanoparticles.” *Asian Journal of Pharmaceutical Sciences* 10 (4): 275–82. https://doi.org/https://doi.org/10.1016/j.ajps.2014.12.007.

Liu, Weilin, Aiqian Ye, Wei Liu, Chengmei Liu, Jianzhong Han, and Harjinder Singh. 2015. “Behaviour of Liposomes Loaded with Bovine Serum Albumin during in Vitro Digestion.” *Food Chemistry* 175 (May): 16–24. https://doi.org/10.1016/j.foodchem.2014.11.108.

Lundstrom, Kenneth, and Teni Boulikas. 2003. “Viral and Non-Viral Vectors in Gene Therapy: Technology Development and Clinical Trials.” *Technology in Cancer Research & Treatment* 2 (5): 471–86. https://doi.org/10.1177/153303460300200513.

Masarudin, Mas Jaffri, Suzanne M Cutts, Benny J Evison, Don R Phillips, and Paul J Pigram. 2015. “Factors Determining the Stability, Size Distribution, and Cellular Accumulation of Small, Monodisperse CS Nanoparticles as Candidate Vectors for Anticancer Drug Delivery: Application to the Passive Encapsulation of [(14)C]-Doxorubicin.” *Nanotechnology, Science and Applications* 8: 67–80. https://doi.org/10.2147/NSA.S91785.

Mohammed, Munawar A, Jaweria T M Syeda, Kishor M Wasan, and Ellen K Wasan. 2017. “An Overview of CS Nanoparticles and Its Application in Non-Parenteral Drug Delivery.” *Pharmaceutics* 9 (4). https://doi.org/10.3390/pharmaceutics9040053.

Nagai, Hiroki, and Young Hak Kim. 2017. “Cancer Prevention from the Perspective of Global Cancer Burden Patterns.” *Journal of Thoracic Disease*. https://doi.org/10.21037/jtd.2017.02.75.

Nayerossadat, Nouri, Talebi Maedeh, and Palizban Abas Ali. 2012. “Viral and Nonviral Delivery Systems for Gene Delivery.” *Advanced Biomedical Research* 1: 27. https://doi.org/10.4103/2277-9175.98152.

Netsomboon, Kesinee, and Andreas Bernkop-Schnürch. 2016. “Mucoadhesive vs. Mucopenetrating Particulate Drug Delivery.” *European Journal of Pharmaceutics and Biopharmaceutics* 98: 76–89.

https://doi.org/https://doi.org/10.1016/j.ejpb.2015.11.003.

Nunes, Renato, Ângela Sousa, Aiva Simaite, Ahmed Aido, and Matej Buzgo. 2021. "Sub-100 Nm CS-Triphosphate-DNA Nanoparticles for Delivery of DNA Vaccines." *Proceedings* 78 (1). https://doi.org/10.3390/IECP2020-08653.

Okuda, K, K Q Xin, A Haruki, S Kawamoto, Y Kojima, F Hirahara, H Okada, D Klinman, and K Hamajima. 2001. "Transplacental Genetic Immunization after Intravenous Delivery of Plasmid DNA to Pregnant Mice." *Journal of Immunology (Baltimore, Md. : 1950)* 167 (9): 5478–84. https://doi.org/10.4049/jimmunol.167.9.5478.

Omar Zaki, Siti Sarah, Mohd Nazmi Ibrahim, and Haliza Katas. 2015. "Particle Size Affects Concentration-Dependent Cytotoxicity of CS Nanoparticles towards Mouse Hematopoietic Stem Cells." Edited by Paresh Chandra Ray. *Journal of Nanotechnology* 2015: 919658. https://doi.org/10.1155/2015/919658.

Özbaş-Turan, Suna, and Jülide Akbuğa. 2011. "Plasmid DNA-Loaded CS/TPP Nanoparticles for Topical Gene Delivery." *Drug Delivery* 18 (3): 215–22. https://doi.org/10.3109/10717544.2010.544688.

Padmanabhan, Swathi, Tahir Amin, Bhaven Sampat, Robert Cook-Deegan, and Subhashini Chandrasekharan. 2010. "Intellectual Property, Technology Transfer and Manufacture of Low-Cost HPV Vaccines in India." *Nature Biotechnology* 28 (7): 671–78. https://doi.org/10.1038/nbt0710-671.

Pal, Asmita, and Rita Kundu. 2019. "Human Papillomavirus E6 and E7: The Cervical Cancer Hallmarks and Targets for Therapy." *Frontiers in Microbiology* 10: 3116. https://doi.org/10.3389/fmicb.2019.03116.

Panyam, Jayanth, and Vinod Labhasetwar. 2003. "Biodegradable Nanoparticles for Drug and Gene Delivery to Cells and Tissue." *Advanced Drug Delivery Reviews* 55 (3): 329–47. https://doi.org/10.1016/s0169-409x(02)00228-4.

Patra, Jayanta Kumar, Gitishree Das, Leonardo Fernandes Fraceto, Estefania Vangelie Ramos Campos, Maria del Pilar Rodriguez-Torres, Laura Susana Acosta-Torres, Luis Armando Diaz-Torres, et al. 2018. "Nano Based Drug Delivery Systems: Recent Developments and Future Prospects." *Journal of Nanobiotechnology* 16 (1): 71. https://doi.org/10.1186/s12951-018-0392-8.

Payne, Susan. 2017. "Chapter 32 - Family Papillomaviridae." In *Viruses*, edited by Susan Payne, 253–59. Academic Press. https://doi.org/https://doi.org/10.1016/B978-0-12-803109-4.00032-5.

Pedroso-Santana, Seidy, and Noralvis Fleitas-Salazar. 2020. "Ionotropic Gelation Method in the Synthesis of Nanoparticles/Microparticles for Biomedical

Purposes." *Polymer International* 69 (5): 443–47. https://doi.org/https://doi.org/10.1002/pi.5970.

Porter, Kevin R, and Kanakatte Raviprakash. 2017. "DNA Vaccine Delivery and Improved Immunogenicity." *Current Issues in Molecular Biology* 22: 129–38. https://doi.org/10.21775/cimb.022.129.

Pudlarz, Agnieszka, and Janusz Szemraj. 2018. "Nanoparticles as Carriers of Proteins, Peptides and Other Therapeutic Molecules." *Open Life Sciences* 13 (1): 285–98. https://doi.org/doi:10.1515/biol-2018-0035.

Raik, Sergei V, Stanislav Andranovitš, Valentina A Petrova, Yingying Xu, Jenny Ka-Wing Lam, Gordon A Morris, Alexandra V Brodskaia, Luca Casettari, Andreii S Kritchenkov, and Yury A Skorik. 2018. "Comparative Study of Diethylaminoethyl-CS and Methylglycol-CS as Potential Non-Viral Vectors for Gene Therapy." *Polymers* 10 (4). https://doi.org/10.3390/polym10040442.

Ramamoorth, Murali, and Aparna Narvekar. 2015. "Non Viral Vectors in Gene Therapy- an Overview." *Journal of Clinical and Diagnostic Research : JCDR* 9 (1): GE01-6. https://doi.org/10.7860/JCDR/2015/10443.5394.

Rampino, Antonio, Massimiliano Borgogna, Paolo Blasi, Barbara Bellich, and Attilio Cesàro. 2013. "CS Nanoparticles: Preparation, Size Evolution and Stability." *International Journal of Pharmaceutics* 455 (1): 219–28. https://doi.org/https://doi.org/10.1016/j.ijpharm.2013.07.034.

Roden, Richard B S, and Peter L Stern. 2018. "Opportunities and Challenges for Human Papillomavirus Vaccination in Cancer." *Nature Reviews Cancer* 18 (4): 240–54. https://doi.org/10.1038/nrc.2018.13.

Rodrigues, Susana, Marita Dionísio, Carmen Remuñán López, and Ana Grenha. 2012. "Biocompatibility of CS Carriers with Application in Drug Delivery." *Journal of Functional Biomaterials* . https://doi.org/10.3390/jfb3030615.

Saad, Maha, Olga B Garbuzenko, Elizabeth Ber, Pooja Chandna, Jayant J Khandare, Vitaly P Pozharov, and Tamara Minko. 2008. "Receptor Targeted Polymers, Dendrimers, Liposomes: Which Nanocarrier Is the Most Efficient for Tumor-Specific Treatment and Imaging?" *Journal of Controlled Release : Official Journal of the Controlled Release Society* 130 (2): 107–14. https://doi.org/10.1016/j.jconrel.2008.05.024.

Santos-Carballal, Beatriz, Elena Fernández Fernández, and Francisco M Goycoolea. 2018. "CS in Non-Viral Gene Delivery: Role of Structure, Characterization Methods, and Insights in Cancer and Rare Diseases Therapies." *Polymers* . https://doi.org/10.3390/polym10040444.

Santos, João, Fani Sousa, João Queiroz, and Diana Costa. 2014. "Rhodamine Based Plasmid DNA Nanoparticles for Mitochondrial Gene Therapy." *Colloids and Surfaces. B, Biointerfaces* 121 (September): 129–40. https://doi.org/10.1016/j.colsurfb.2014.06.003.

Silva, Sara Baptista da, Manuela Amorim, Pedro Fonte, Raquel Madureira, Domingos Ferreira, Manuela Pintado, and Bruno Sarmento. 2015. "Natural Extracts into CS Nanocarriers for Rosmarinic Acid Drug Delivery." *Pharmaceutical Biology* 53 (5): 642–52. https://doi.org/10.3109/13880209.2014.935949.

Sinha, Vivek Ranjan, Saurabh Srivastava, Honey Goel, and Vinay Jindal. 2011. "Solid Lipid Nanoparticles (SLN'S) – Trends and Implications in Drug Targeting." *International Journal of Advances in Pharmaceutical Sciences; Vol 1, No 3 (2010): International Journal of Advances in Pharmaceutical Sciences*. https://www.arjournals.org/index.php/ijaps/article/view/172.

Smith, Herbert A, and Dennis M Klinman. 2001. "The Regulation of DNA Vaccines." *Current Opinion in Biotechnology* 12 (3): 299–303. https://doi.org/https://doi.org/10.1016/S0958-1669(00)00215-9.

Sousa, Hugo, Ana Tavares, Carla Campos, Joana Marinho-Dias, Margarida Brito, Rui Medeiros, Inês Baldaque, et al. 2019. "High-Risk Human Papillomavirus Genotype Distribution in the Northern Region of Portugal: Data from Regional Cervical Cancer Screening Program." *Papillomavirus Research (Amsterdam, Netherlands)* 8 (December): 100179. https://doi.org/10.1016/j.pvr.2019.100179.

Sreekumar, Sruthi, Francisco M Goycoolea, Bruno M Moerschbacher, and Gustavo R Rivera-Rodriguez. 2018. "Parameters Influencing the Size of CS-TPP Nano- and Microparticles." *Scientific Reports* 8 (1): 4695. https://doi.org/10.1038/s41598-018-23064-4.

Subhashis Debnath, R. Suresh Kumar, M. Niranjan Babu. 2011. "Ionotropic Gelation – A Novel Method to Prepare CS Nanoparticles." *Research J. Pharm. and Tech.* 4(4): 492–95.

Sung, Y K, and S W Kim. 2019. "Recent Advances in the Development of Gene Delivery Systems." *Biomaterials Research* 23 (1): 8. https://doi.org/10.1186/s40824-019-0156-z.

Tian, Jun-Nan, Bing-Qiang Ge, Yun-Feng Shen, Yu-Xuan He, and Zhong-Xiu Chen. 2016. "Thermodynamics and Structural Evolution during a Reversible Vesicle-Micelle Transition of a Vitamin-Derived Bolaamphiphile Induced by Sodium Cholate." *Journal of Agricultural and Food Chemistry* 64 (9): 1977–88. https://doi.org/10.1021/acs.jafc.5b05547.

Torchilin, Vladimir P. 2005. “Recent Advances with Liposomes as Pharmaceutical Carriers.” *Nature Reviews Drug Discovery* 4 (2): 145–60. https://doi.org/10.1038/nrd1632.

Tzeyung, Angeline Shak., Shadab Md, Subrat Kumar Bhattamisra, Thiagarajan Madheswaran, Nabil A Alhakamy, Hibah M Aldawsari, and Ammu K Radhakrishnan. 2019. “Fabrication, Optimization, and Evaluation of Rotigotine-Loaded CS Nanoparticles for Nose-To-Brain Delivery.” *Pharmaceutics* 11 (1). https://doi.org/10.3390/pharmaceutics11010026.

Valente, J F A, P Pereira, A Sousa, J A Queiroz, and F Sousa. 2021. “Effect of Plasmid DNA Size on CS or Polyethyleneimine Polyplexes Formulation.” *Polymers* 13 (5). https://doi.org/10.3390/polym13050793.

Viarisio, Daniele, Lutz Gissmann, and Massimo Tommasino. 2017. “Human Papillomaviruses and Carcinogenesis: Well-Established and Novel Models.” *Current Opinion in Virology* 26 (October): 56–62. https://doi.org/10.1016/j.coviro.2017.07.014.

Walters, Adam A, Christos Krastev, Adrian V S Hill, and Anita Milicic. 2015. “Next Generation Vaccines: Single-Dose Encapsulated Vaccines for Improved Global Immunisation Coverage and Efficacy.” *The Journal of Pharmacy and Pharmacology* 67 (3): 400–408. https://doi.org/10.1111/jphp.12367.

Wang, Joshua W, and Richard B S Roden. 2013. “Virus-like Particles for the Prevention of Human Papillomavirus-Associated Malignancies.” *Expert Review of Vaccines* 12 (2): 129–41. https://doi.org/10.1586/erv.12.151.

Wang, Liping, Wenhua Zhang, Quan Zhou, Shihai Liu, Wenhua Xu, Teng Sun, and Ye Liang. 2018. “Establishing Gene Delivery Systems Based on Small-Sized CS Nanoparticles.” *Journal of Ocean University of China* 17 (5): 1253–60. https://doi.org/10.1007/s11802-018-3658-8.

Whiteley, Zoe, Hei Ming Kenneth Ho, Yee Xin Gan, Luca Panariello, Georgios Gkogkos, Asterios Gavriilidis, and Duncan Q M Craig. 2021. “Microfluidic Synthesis of Protein-Loaded Nanogels in a Coaxial Flow Reactor Using a Design of Experiments Approach.” *Nanoscale Adv.* 3 (7): 2039–55. https://doi.org/10.1039/D0NA01051K.

Wu, Wei, Yi Lu, and Jianping Qi. 2015. “Oral Delivery of Liposomes.” *Therapeutic Delivery* 6 (11): 1239–41. https://doi.org/10.4155/tde.15.69.

Xu, Yingying, Pak-Wai Yuen, and Jenny Ka-Wing Lam. 2014. “Intranasal DNA Vaccine for Protection against Respiratory Infectious Diseases: The Delivery Perspectives.” *Pharmaceutics* 6 (3): 378–415. https://doi.org/10.3390/pharmaceutics6030378.

Yim, Eun-Kyoung, and Jong-Sup Park. 2005. “The Role of HPV E6 and E7 Oncoproteins in HPV-Associated Cervical Carcinogenesis.” *Cancer Research and Treatment* 37 (6): 319–24. https://doi.org/10.4143/crt.2005.37.6.319.

Zhang, Ke, Huafeng Fang, Zhiyun Chen, John-Stephen A Taylor, and Karen L Wooley. 2008. “Shape Effects of Nanoparticles Conjugated with Cell-Penetrating Peptides (HIV Tat PTD) on CHO Cell Uptake.” *Bioconjugate Chemistry* 19 (9): 1880–87. https://doi.org/10.1021/bc800160b.

7 Annexes

Figure 25. Video-Presentation submitted to the 1st International Electronic Conference on Pharmaceutics (IECP 2020).

Open Access Proceedings

Sub-100 nm Chitosan-Triphosphate-DNA Nanoparticles for Delivery of DNA Vaccines †

by Renato Nunes [1,2,*], Ângela Sousa [1], Aiva Simaite [2], Ahmed Aido [2] and Matej Buzgo [2]

[1] CICS-UBI—Health Sciences Research Center, University of Beira Interior, Avenida Infante D Henrique, 6200-506 Covilhã, Portugal

[2] InoCure s.r.o, R&D Lab, Prumyslová 1980, 250 88 Celákovice, Czech Republic

* Author to whom correspondence should be addressed.

† Presented at the 1st International Electronic Conference on Pharmaceutics, 1–15 December 2020; Available online: https://iecp2020.sciforum.net/.

Proceedings **2021**, *78*(1), 12; https://doi.org/10.3390/IECP2020-08653

Published: **1 December 2020**

(This article belongs to the Proceedings of The 1st International Electronic Conference on Pharmaceutics)

Download PDF Citation Export

Abstract

Intramuscular delivery is one of the main routes for DNA vaccines administration. However, it requires large amounts of the DNA to be administered and external stimulation to encourage the internalization of the DNA. In this work, we consider alternative routes for less invasive administration and develop drug delivery systems (DDS) for intranasal administration. Chitosan polyplexes using sodium tripolyphosphate (TPP) as a crosslinker were prepared using the ionic gelation method. Our method allowed preparation of nanoparticles with the size below 50 nm, which is at least two times lower than previously reported sizes. Moreover, despite the small sizes, we obtained DNA encapsulation efficiencies of about 70%. Parameters that may affect the encapsulation efficiency were investigated, including different TPP-chitosan ratios and concentrations of DNA. We found that encapsulation efficiency of DNA inside the particles decreases with the increasing TPP-chitosan ratio. Moreover, increasing the DNA concentration leads to a higher encapsulation efficiency. Small (<50 nm) chitosan nanoparticles hold enormous potential as DNA carriers due to their physiological barriers and subsequent internalization.

Keywords: chitosan; DNA vaccines; tripolyphosphate; nanoparticles; ionic gelation

Figure 26. Scientific article submitted and accepted by MPDI/Proceedings for the 1st International Electronic Conference on Pharmaceutics (IECP 2020).